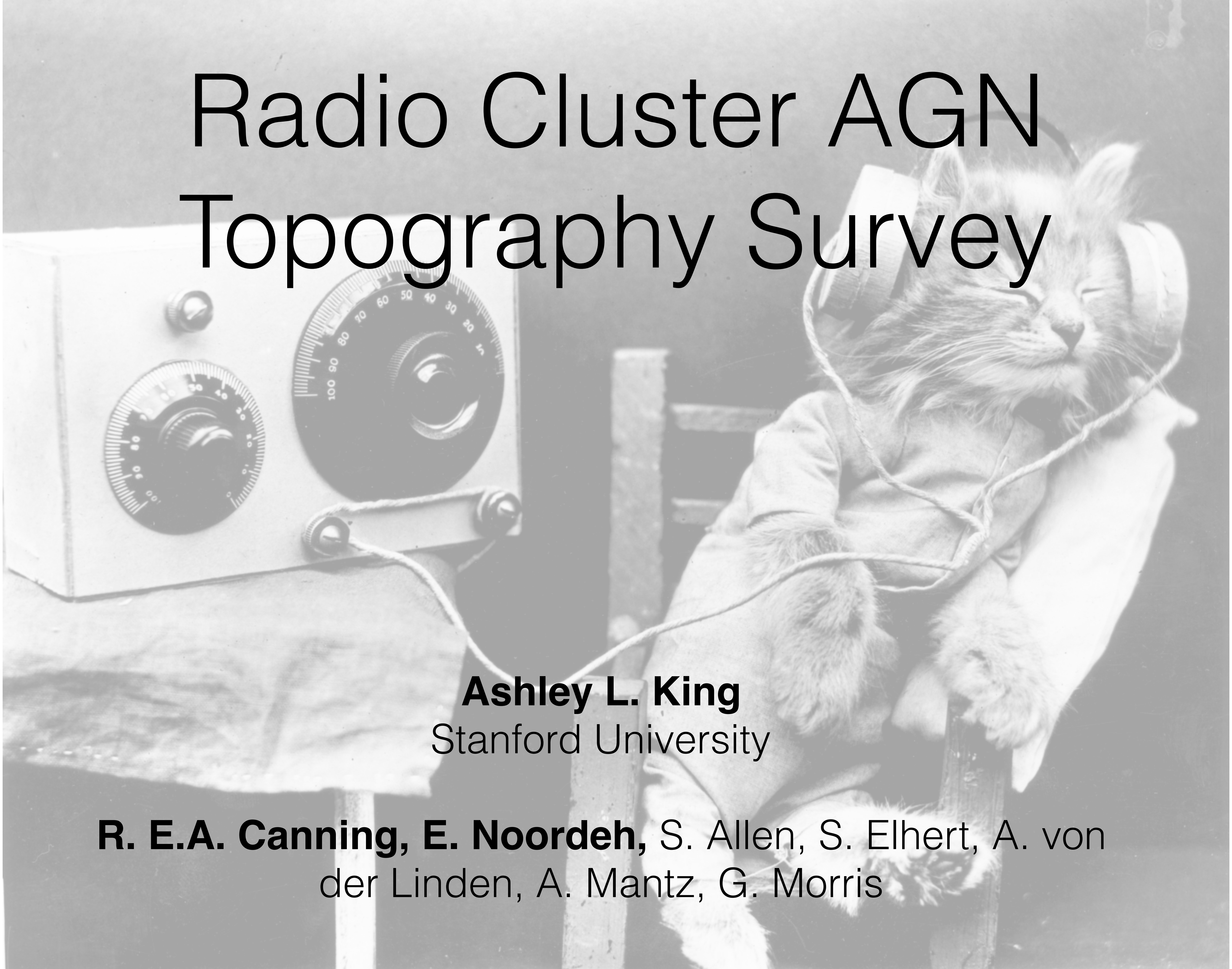

Radio Cluster AGN Topography Survey

Ashley L. King
Stanford University

R. E.A. Canning, E. Noordeh, S. Allen, S. Elhert, A. von der Linden, A. Mantz, G. Morris

Motivation

- **Clusters of Galaxies: great laboratories to examine numerous effects on the host members and their supermassive black holes**

  - **Mergers,**
  - **Mass Segregation,**
  - **Tidal Effects,**
  - **Gas dynamics,**
  - **Shocks,**
  - **Strangulation,**
  - **Gas stripping,**
  - **Cooling Flows**

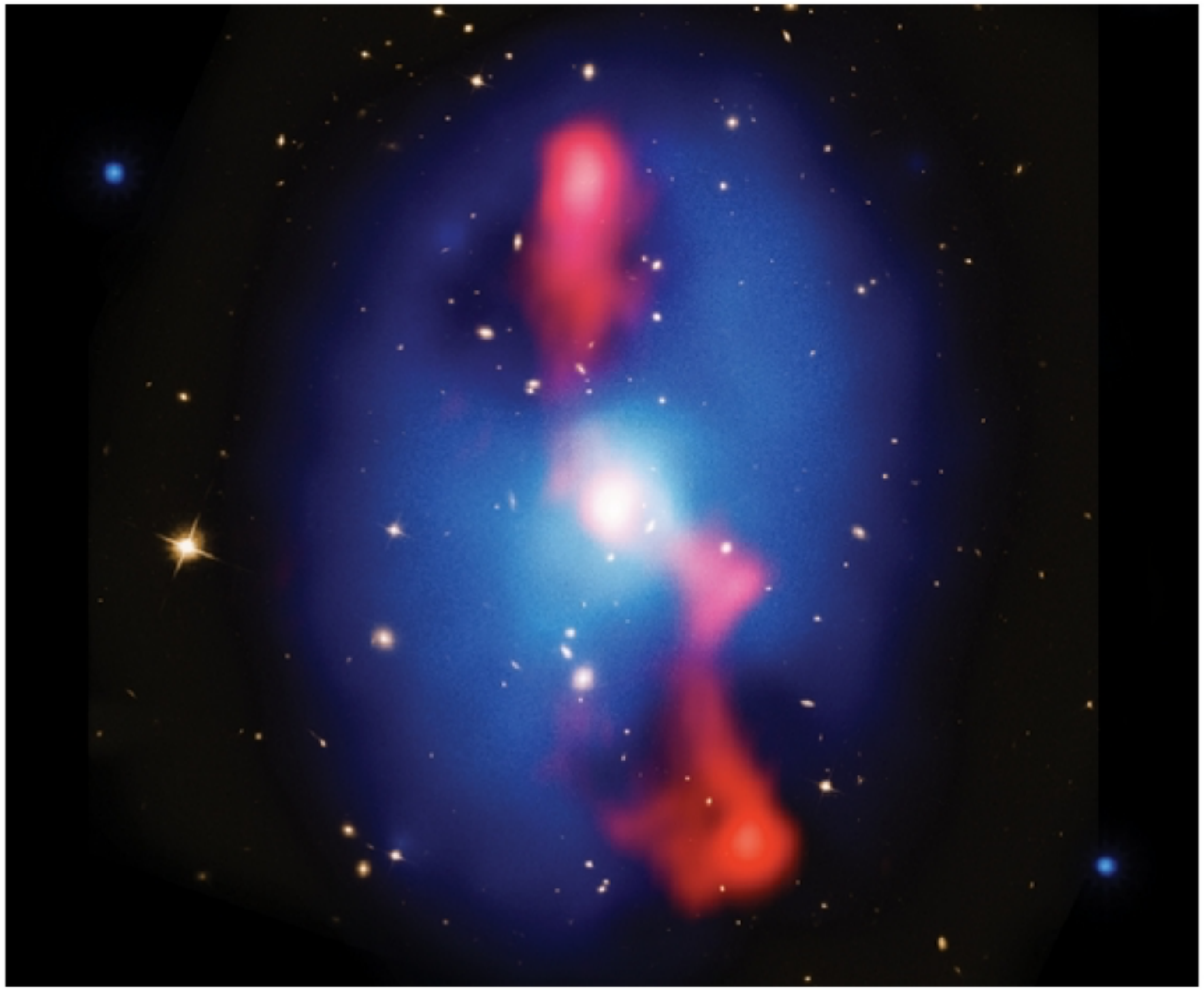

Radio Cluster Sample

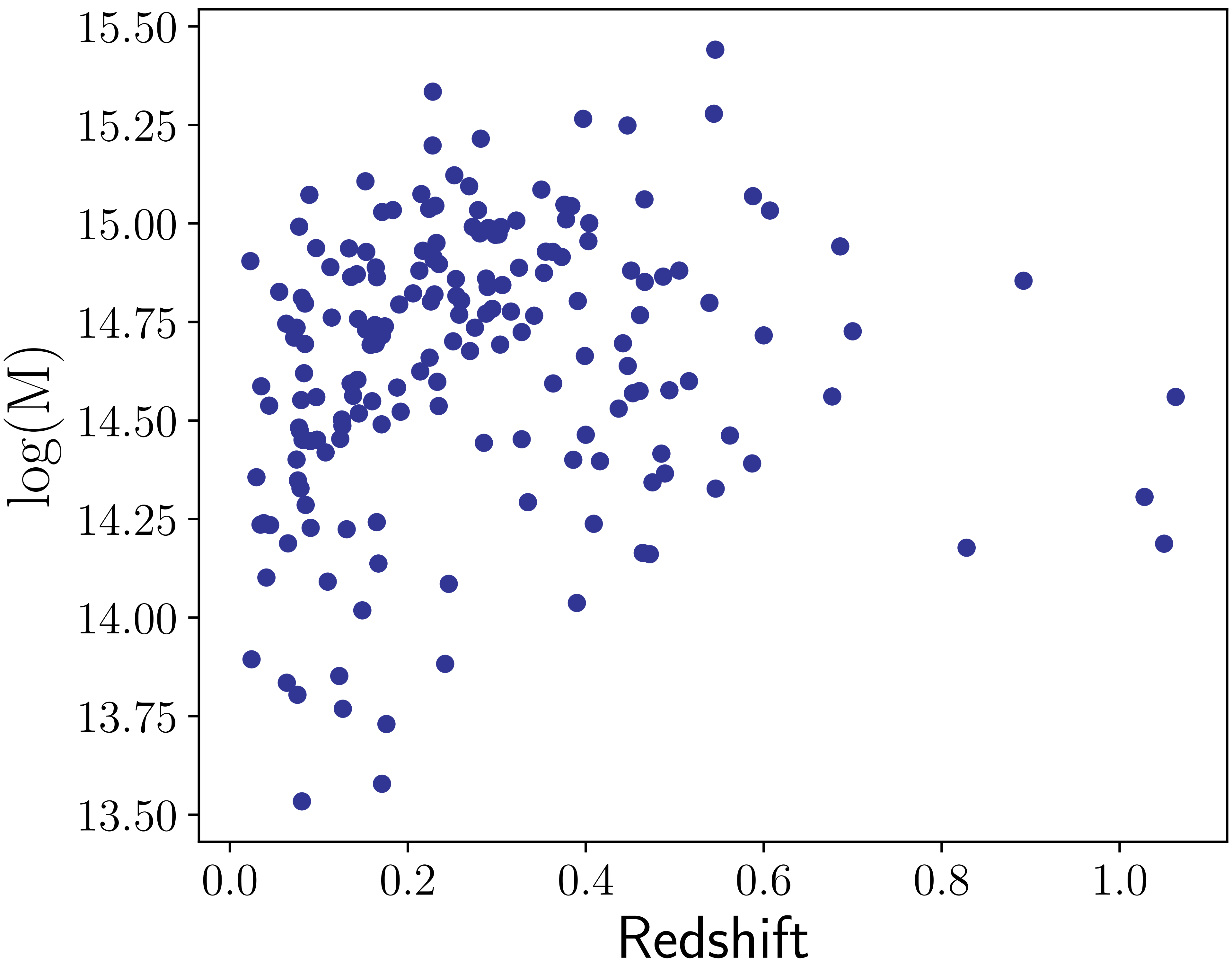

- 183 Clusters in FIRST footprint from our 400+ X-ray CATS sample
  - tripled our sample from last year!!!
- Precise cluster masses and center of masses from high resolution Chandra X-ray observations

FIRST Survey

- FIRST survey - 1.4 GHz VLA
  - S >3 mJy
    - Complete
  - L >10^{23} W/Hz
    - avoid star formation contamination
  - We developed an algorithm to combine multiple components into one source
    - Point Sources
    - Bipolar Outflows
    - Head-Tails
    - Extended emission & Relics

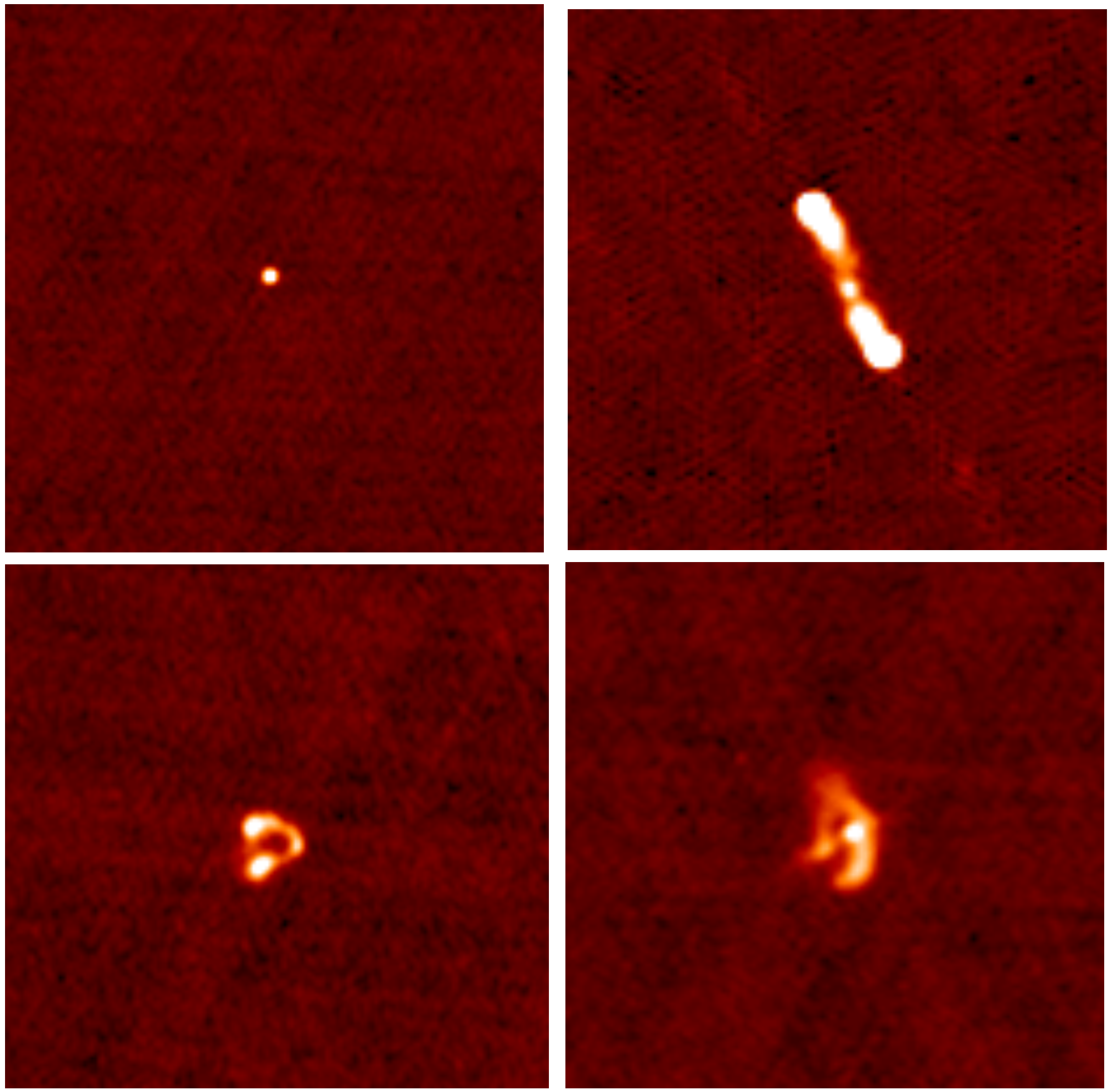

Radio AGN Number Density

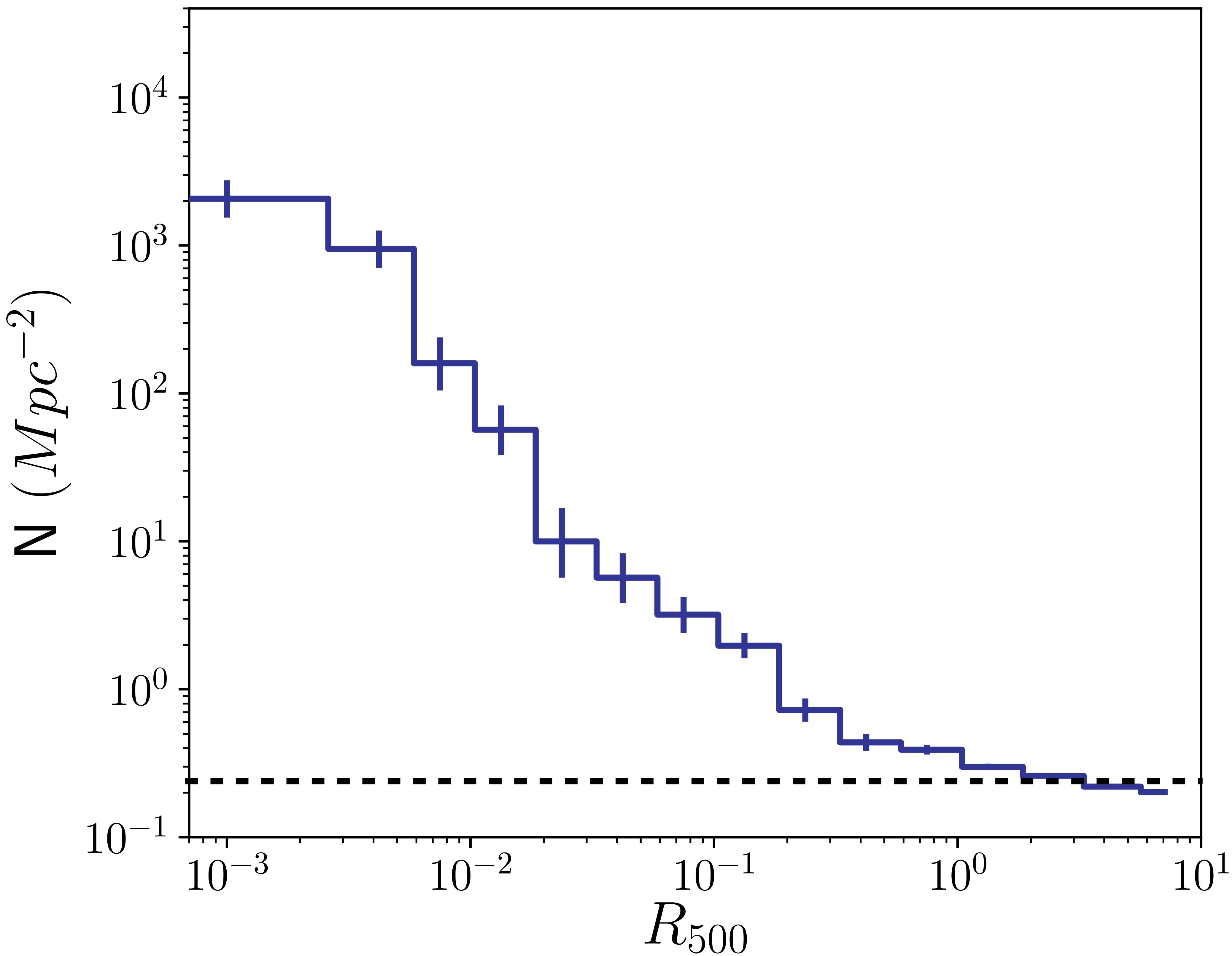

Radio AGN Model

- Differential Analysis to statistically remove the background radio sources

- Inhomogeneous Poisson Spatial Point Process (e.g. Baddeley et al. 2006)

  - We don't bin the data into radius, cluster mass or redshift bins!

  - Probability of the data given particular model parameters

$$\ln P(D|\mu) \propto -\int_0^{R_{max}} \lambda(r|\mu) 2\pi r dr + \sum_{i=0}^{N} \lambda(r_i|\mu)$$

  - Probability of the model given the data and model priors

$$\ln P(\mu|D) \propto -\int \lambda(r) 2\pi r dr + \sum_{i=0}^{N} \lambda(r_i) + \ln P(\mu)$$

    - Use an MCMC to explore this likelihood space

Radio AGN Model

$$\lambda(r) = \left(A_G \Phi_{RLF} \frac{1}{2\pi(\sigma^2+\epsilon^2)} e^{-\frac{r^2}{2(\sigma^2+\epsilon^2)}} + A_\beta \Phi_{RLF} \left(1+\left(\frac{r}{r_c}\right)^2\right)^{-3/2\beta+1/2} \right) \times D_A R_{500}(1+z)^3 + C_{Bkg}$$

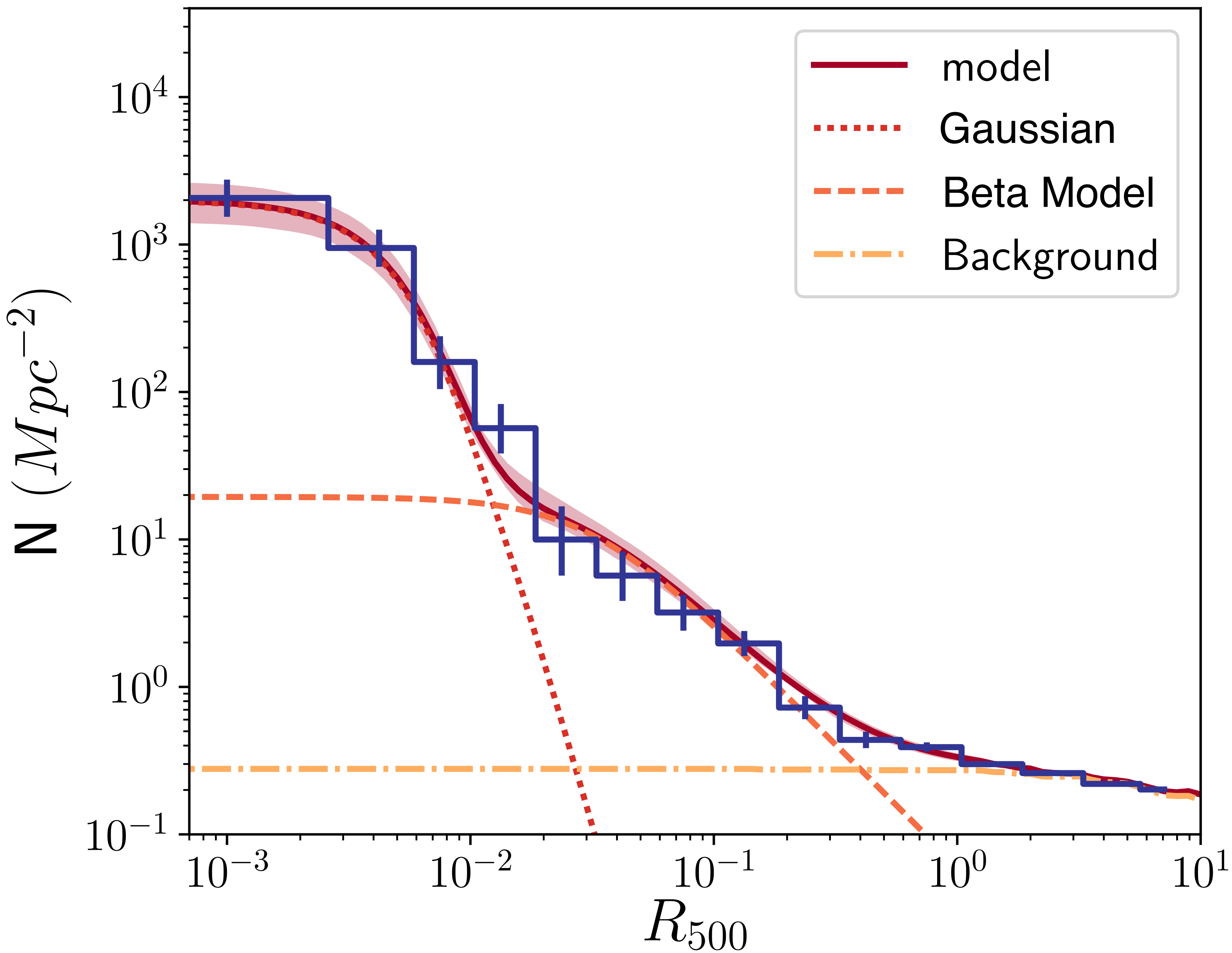

$$\sigma = 2.2 \pm 0.2 \times 10^{-3} R_{500}$$
$$r_c = 2.9^{+1.1}_{-0.6} \times 10^{-2} R_{500}$$
$$\beta = 0.89 \pm 0.05$$

- Cluster is enhancing radio AGN activity over the expected over-density in clusters

$$\langle n_{RAGN} \rangle = f_{500} \frac{500}{\Omega} \Phi_{rlf}$$

f_{500} = 20 +/- 7

- Lin & Mohr 2007 find f_{200} = 6.8 +/- 1.7, suggesting the number density is increasing toward the center

Redshift Evolution

$$\lambda(r) = \left(A_G \Phi_{RLF} \frac{1}{2\pi(\sigma^2+\epsilon^2)} e^{-\frac{r^2}{2(\sigma^2+\epsilon^2)}} + A_\beta \Phi_{RLF} \left(1 + \left(\frac{r}{r_c}\right)^2\right)^{-3/2\beta+1/2} \right) \times D_A R_{500} (1+z)^3 + C_{Bkg}$$

Field RLF from Pracy et al. 2014

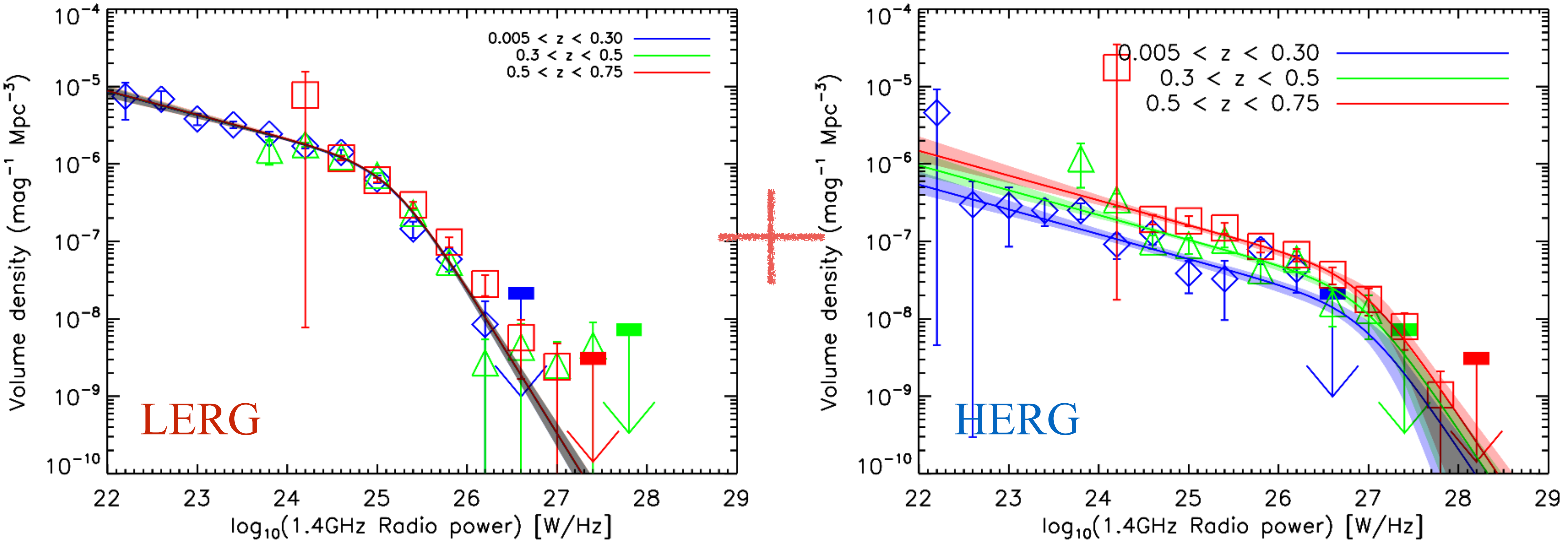

Cluster number density is <u>consistent</u> with the field radio luminosity function redshift evolution

Mass Dependence

$$\lambda(r) = \left(A_G \Phi_{RLF} \frac{1}{2\pi(\sigma^2+\epsilon^2)} e^{-\frac{r^2}{2(\sigma^2+\epsilon^2)}} + A_\beta \Phi_{RLF} \left(1 + \left(\frac{r}{r_c}\right)^2\right)^{-3/2\beta+1/2} \right) \times D_A R_{500} (1+z)^3 + C_{Bkg}$$

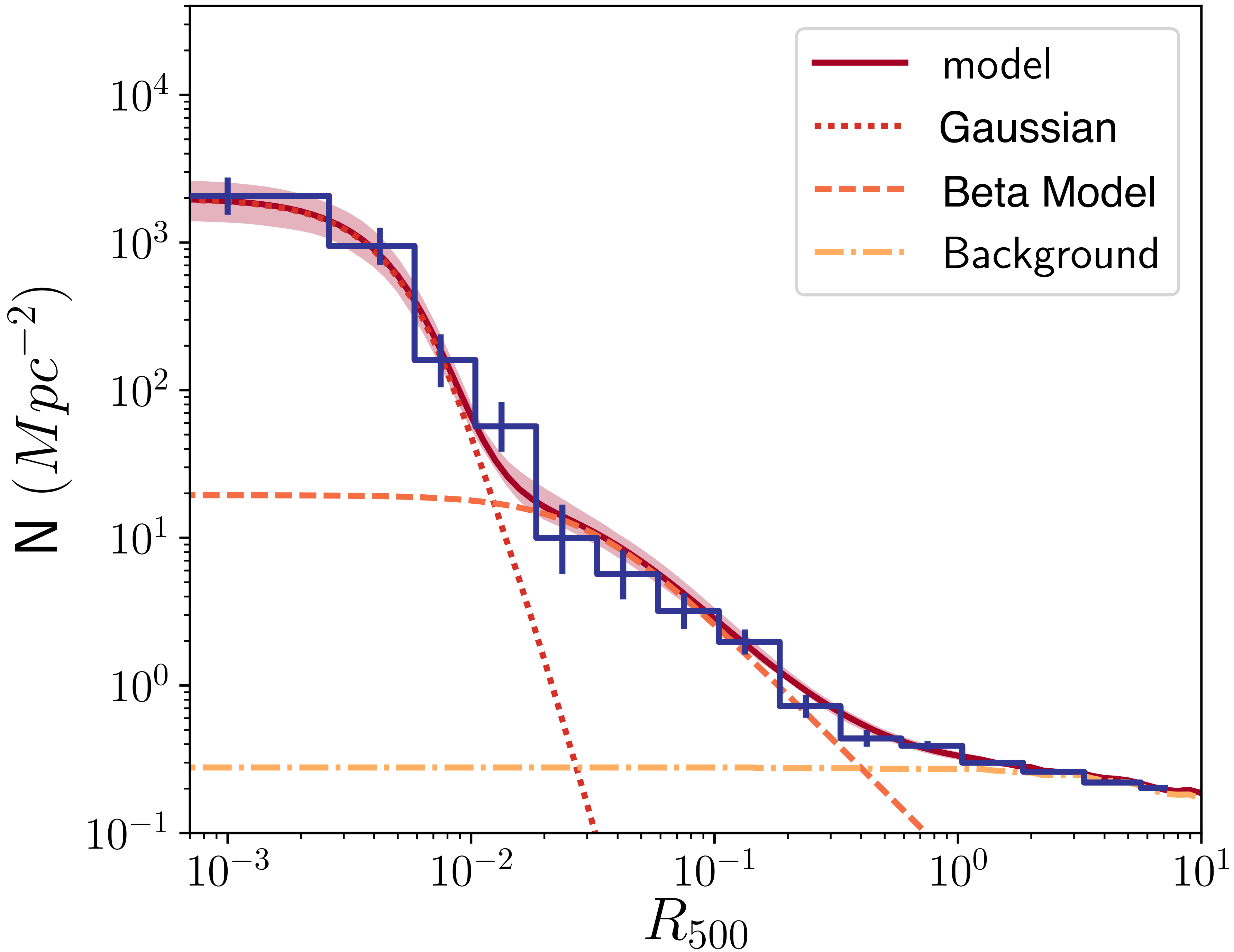

$$A_G = A_{G,0} \left(\frac{M_{500}}{10^{15} M_\odot} \right)^{\alpha_{G,M}}$$

$$A_\beta = A_{\beta,0} \left(\frac{M_{500}}{10^{15} M_\odot} \right)^{\alpha_{\beta,M}}$$

Inverse Mass Dependence

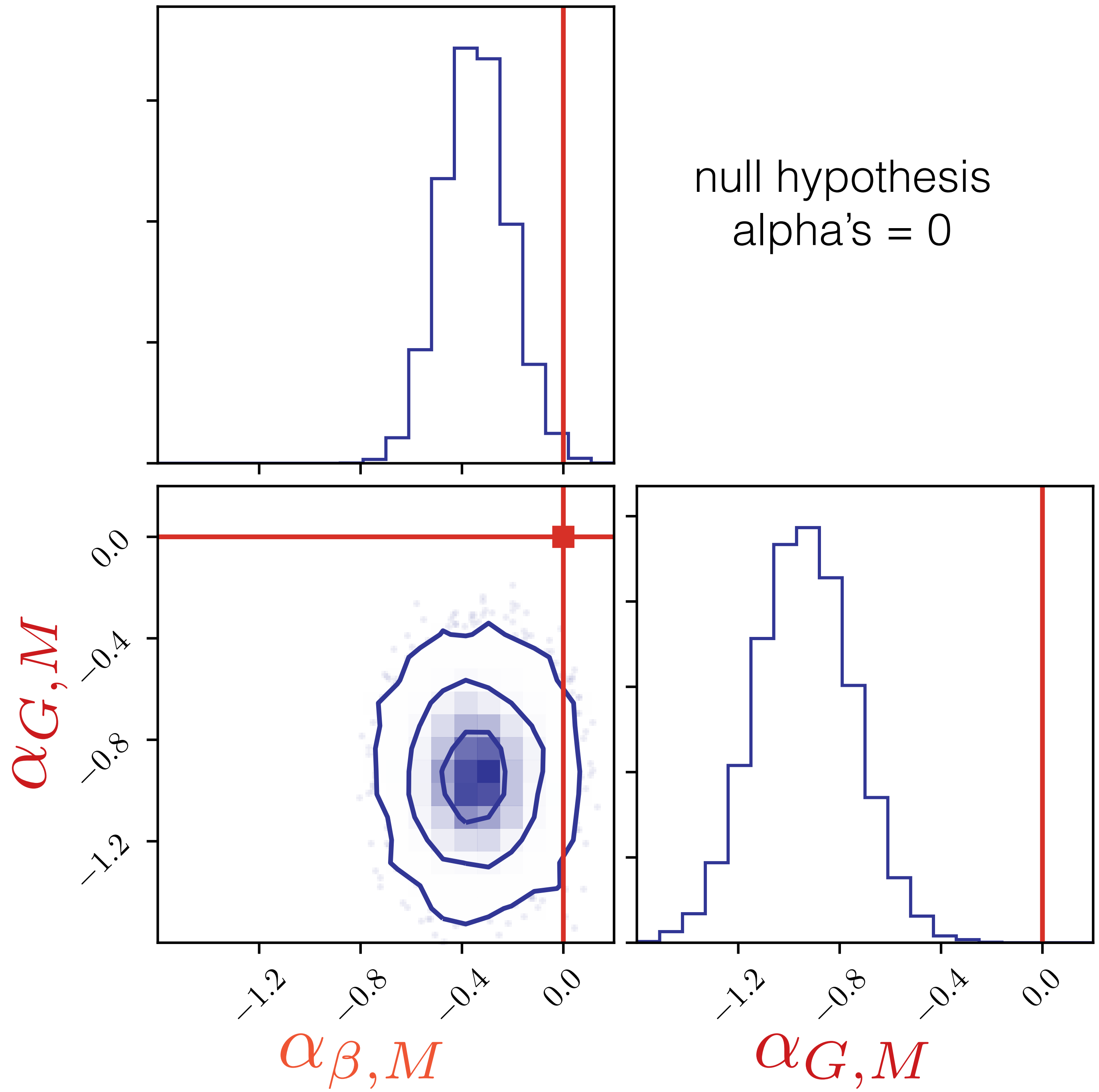

null hypothesis
alpha's = 0

$$A_G = A_{G,0} \left(\frac{M_{500}}{10^{15} M_\odot} \right)^{\alpha_{G,M}}$$

$$A_\beta = A_{\beta,0} \left(\frac{M_{500}}{10^{15} M_\odot} \right)^{\alpha_{\beta,M}}$$

$$\alpha_{G,M} = -0.94 \pm 0.20$$

$$\alpha_{\beta,M} = -0.35 \pm 0.13$$

Inverse Mass Dependence

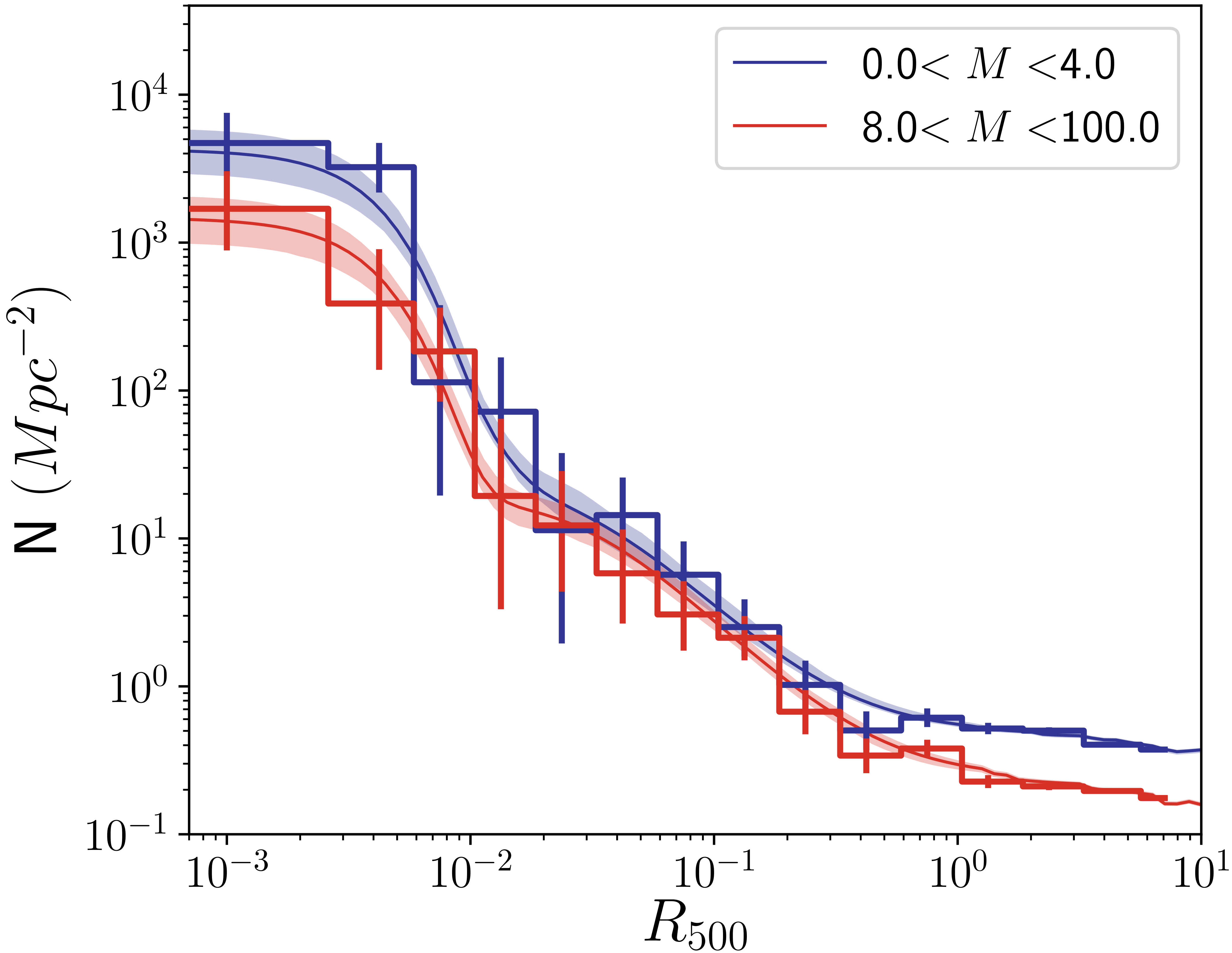

Cooling Flows

- Birzan et al. 2012

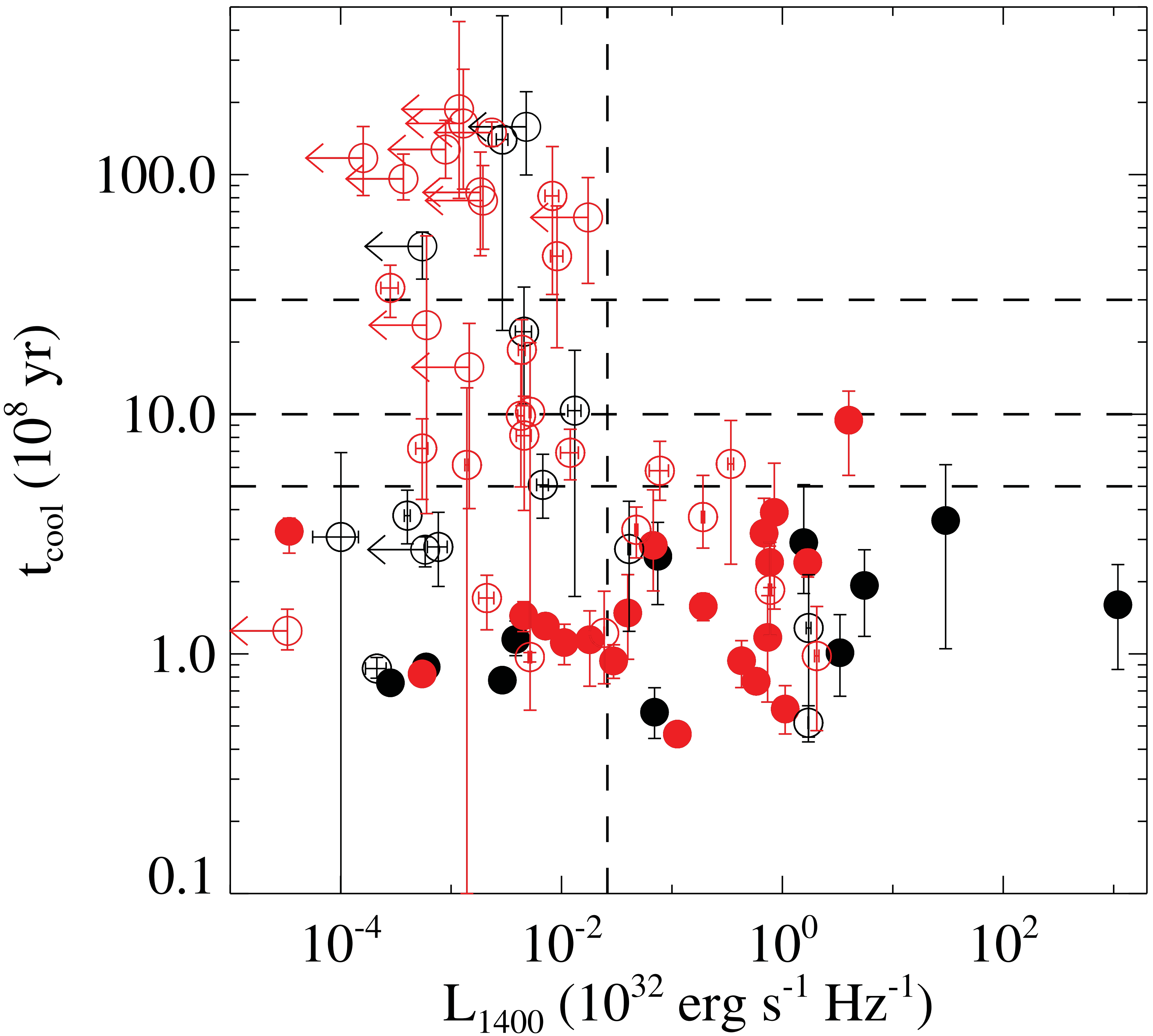

Cooling Flows

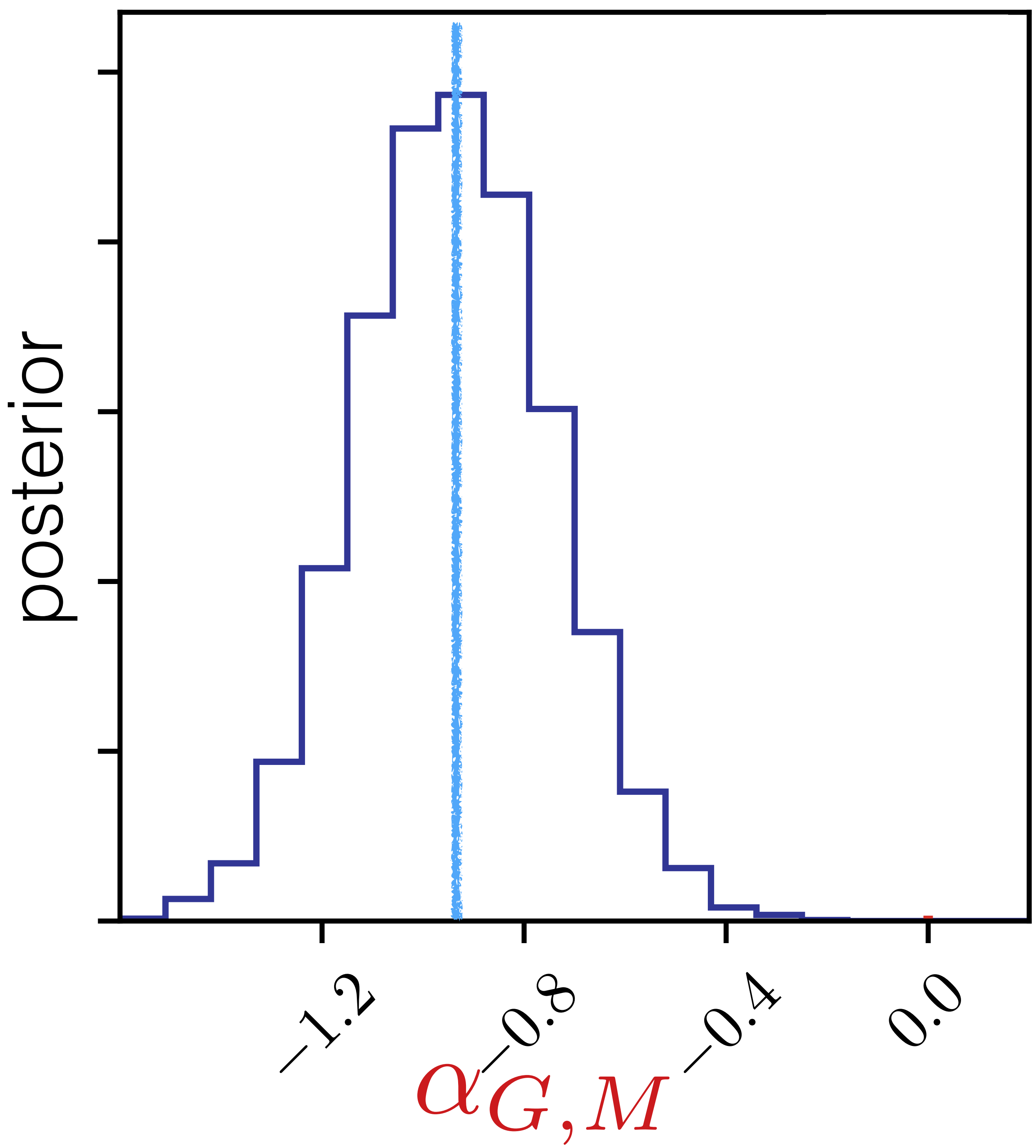

- Cooling timescales

$$t_{cool} \propto \frac{T}{n\Lambda(T)}$$

- BCG is ``on'', N=1, if:

$$t_{cool} << t_{age}$$

- Assume a constant fraction of cool core clusters with mass - Andrade-Santos et al. 2017
  - <N> = constant
- Self-Similar Cluster Scaling

$$M \propto R^3$$

- Number density scales as:

$$\frac{N}{V} \propto \frac{1}{R^3} \propto M^{-1}$$

Inverse Mass Dependence

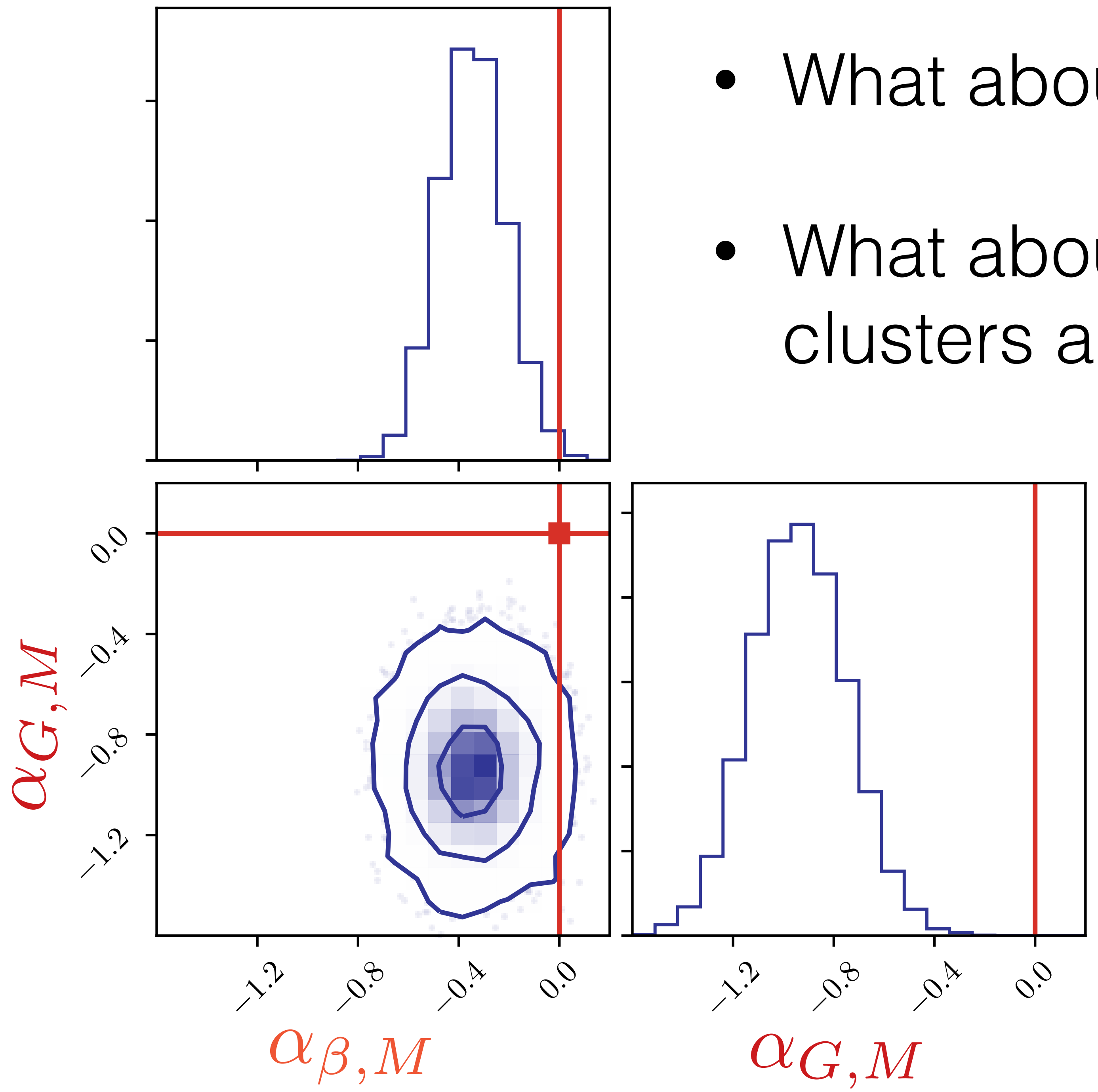

- What about the outskirts?
- What about at higher redshifts when the clusters are not as relaxed?

$$\alpha_{G,M} = -0.94 \pm 0.20$$

$$\alpha_{\beta,M} = -0.35 \pm 0.13$$

Mergers and Tidal Interactions

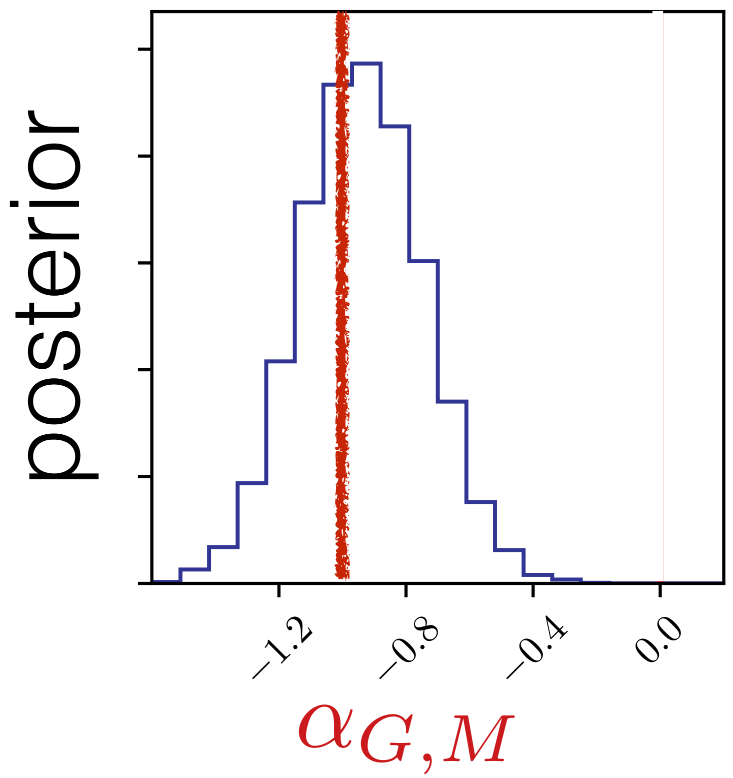

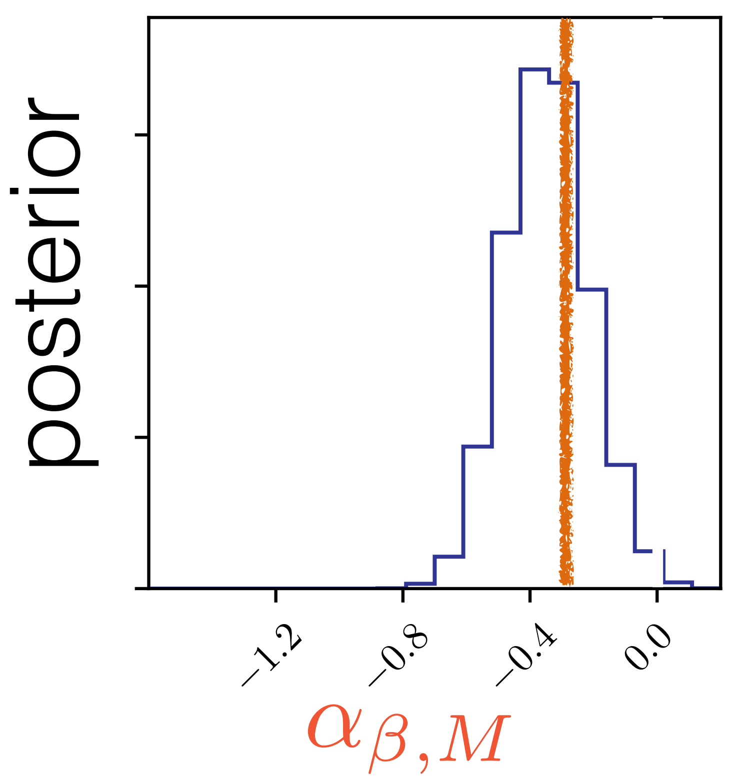

- **Mamon 1992 & 2000**
  - **Merger** rate per galaxy

    $$n\bar{k}_{merger} \propto \sigma^{-3} \propto M^{-1}$$

  - Number density of mergers

    $$\rho_{merger} = n^2\bar{k}_{merger}/H_0 \propto M^{-1}$$

    $$\alpha_{G,M} = -0.94 \pm 0.20$$

  - **Tidal Interaction** rate per galaxy

    $$n\bar{k}_{tidal} \propto \sigma^{-1} \propto M^{-1/3}$$

  - Number density of Tidal Interactions

    $$\rho_{tidal} = n^2\bar{k}_{tidal}/H_0 \propto M^{-1/3}$$

    $$\alpha_{\beta,M} = -0.35 \pm 0.13$$

Mergers and Tidal Interactions

- **Mergers**
  - Centrally concentrated
  - Depends on galaxy mass

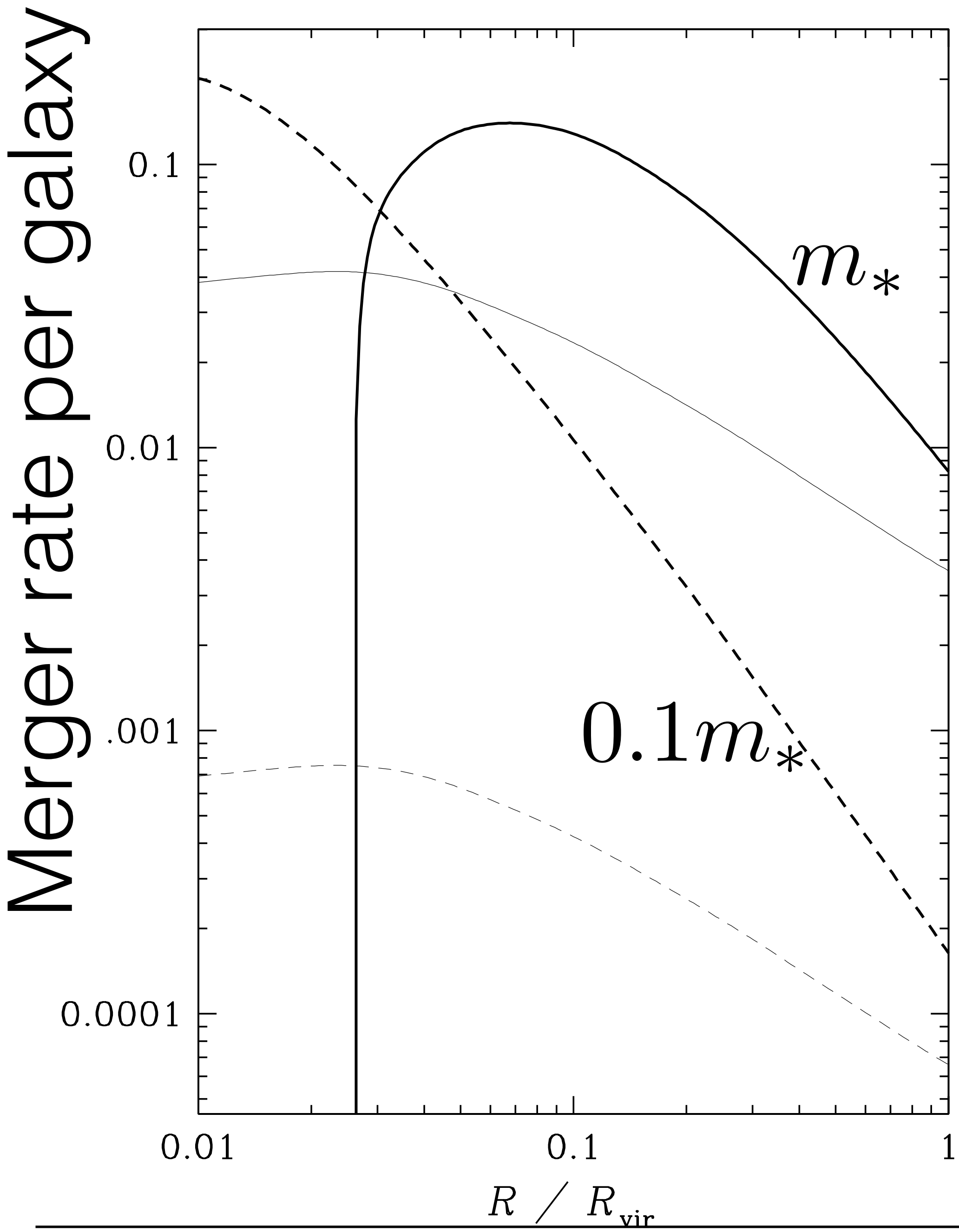

- **Tidal Interactions**
  - Radially increasing
  - galaxy mass independent

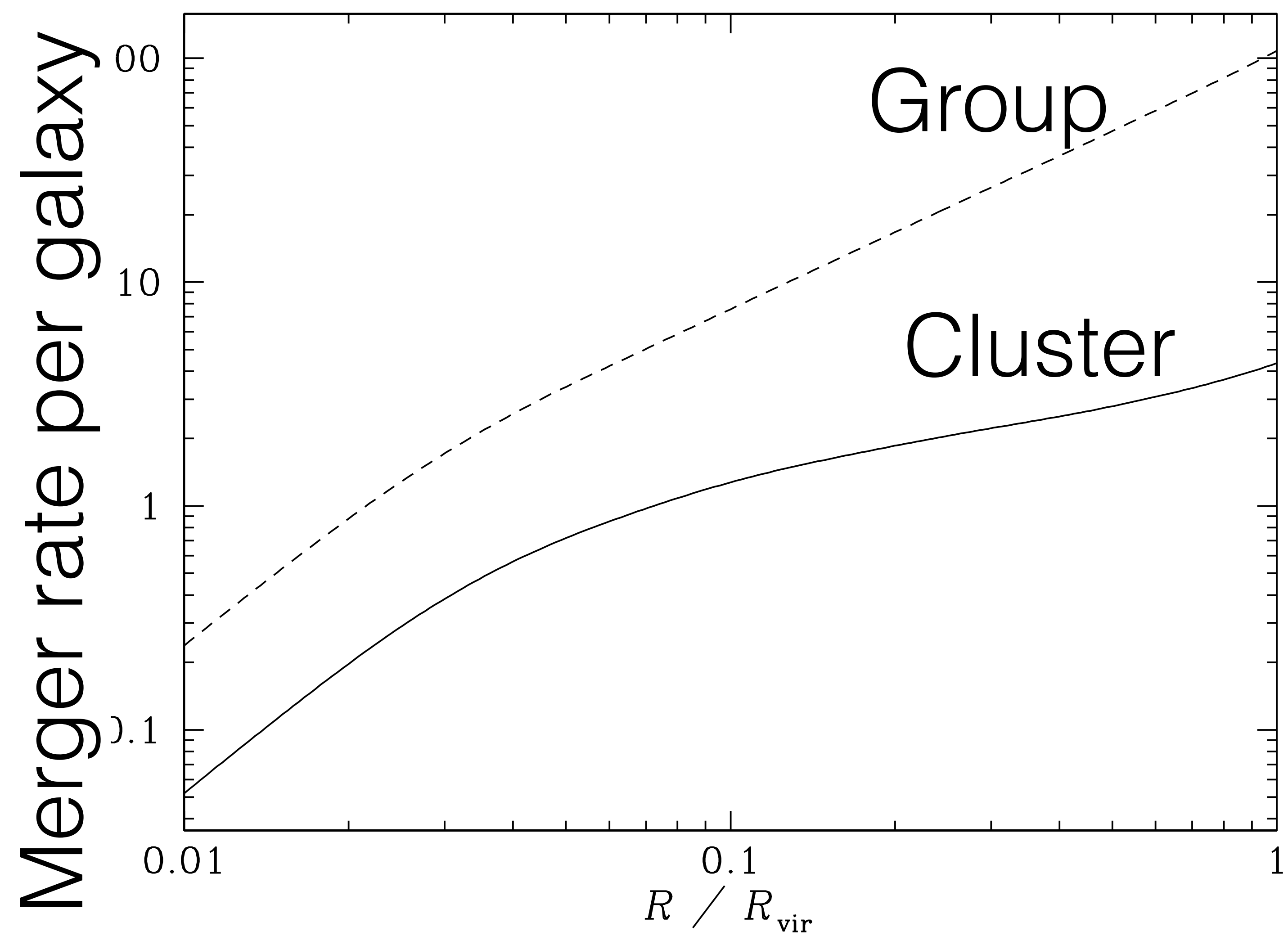

Mamon 2000

Future

- Increase sample size with ATCA observations of SPT clusters, especially to higher redshifts
- Does the number density correlate with:
  - Entropy Profiles
  - Density Profiles
  - Central Cooling times
  - Metallicity

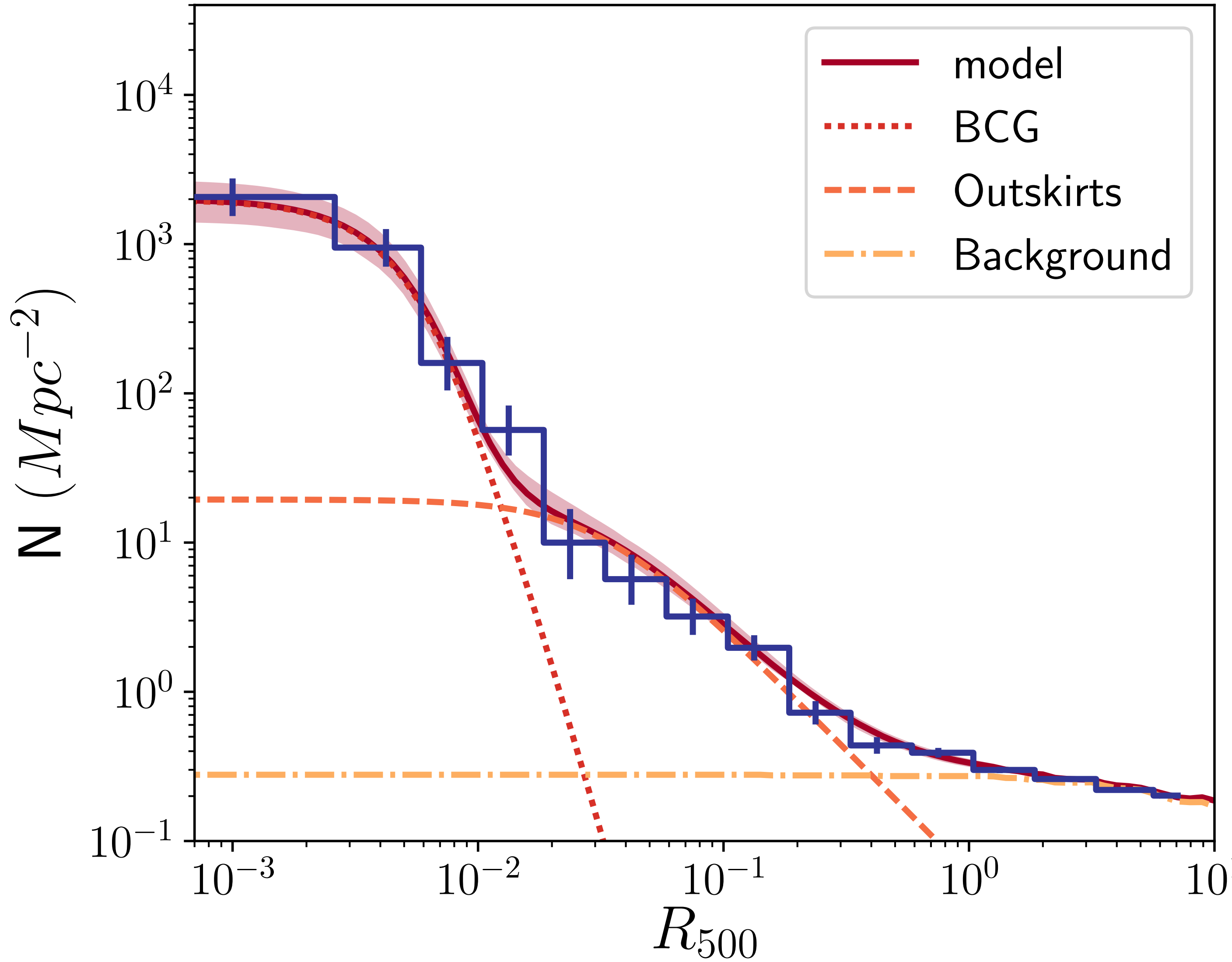

Summary

- Inhomogeneous poisson spatial point process allows us to **not bin** the data!
- We find **two components** best describe the cluster radio AGN number density (Gaussian + Beta Model)
  - Beta model is much steeper than normal galaxy distribution, but consistent with other radio AGN studies (e.g., Girardi et al. 1995, Reddy & Yun 2004, Sommer et al. 2011, Best et al. 12)
- **Redshift evolution is consistent with the field evolution**
  - Sommer et al. 2011 also find a strong redshift evolution that is roughly consistent with the field
- **Inverse cluster mass dependence**
  - Lin & Mohr 2007 find their lower mass bin has a factor of 2 higher number density than their higher mass bin (log $M_{200} > 14.2$)
  - **Gaussian** component number density inversely scales with cluster $\mathbf{M^{-1}}$
    - Consistent with both Cooling Flows and Mergers (Mamon 1992)
  - **Beta Model** component number density inversely scales with cluster $\mathbf{M^{-1/3}}$
    - Consistent with the expected tidal interaction rate (Mamon 2000)

Extra slides

SDSS Colors

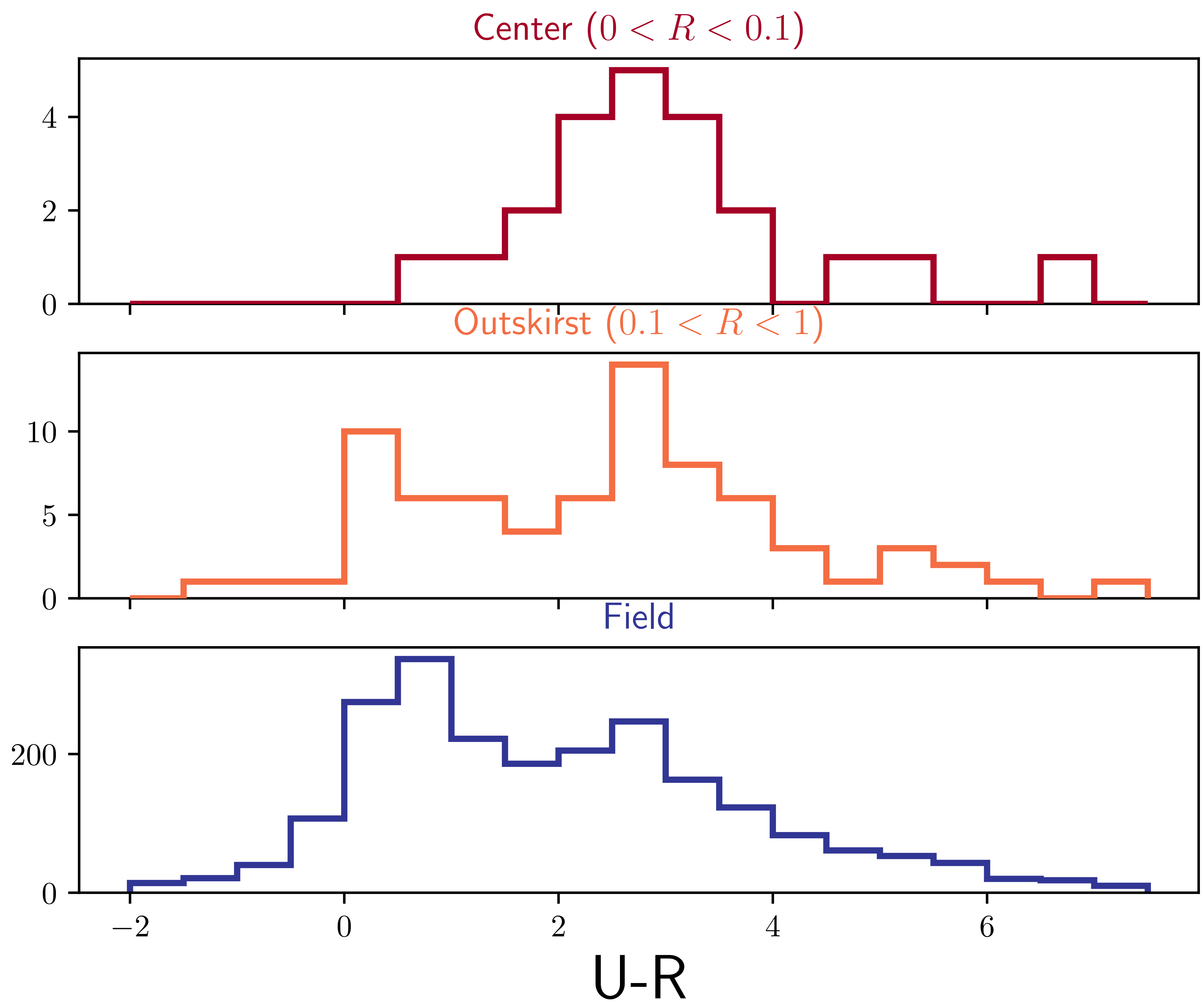

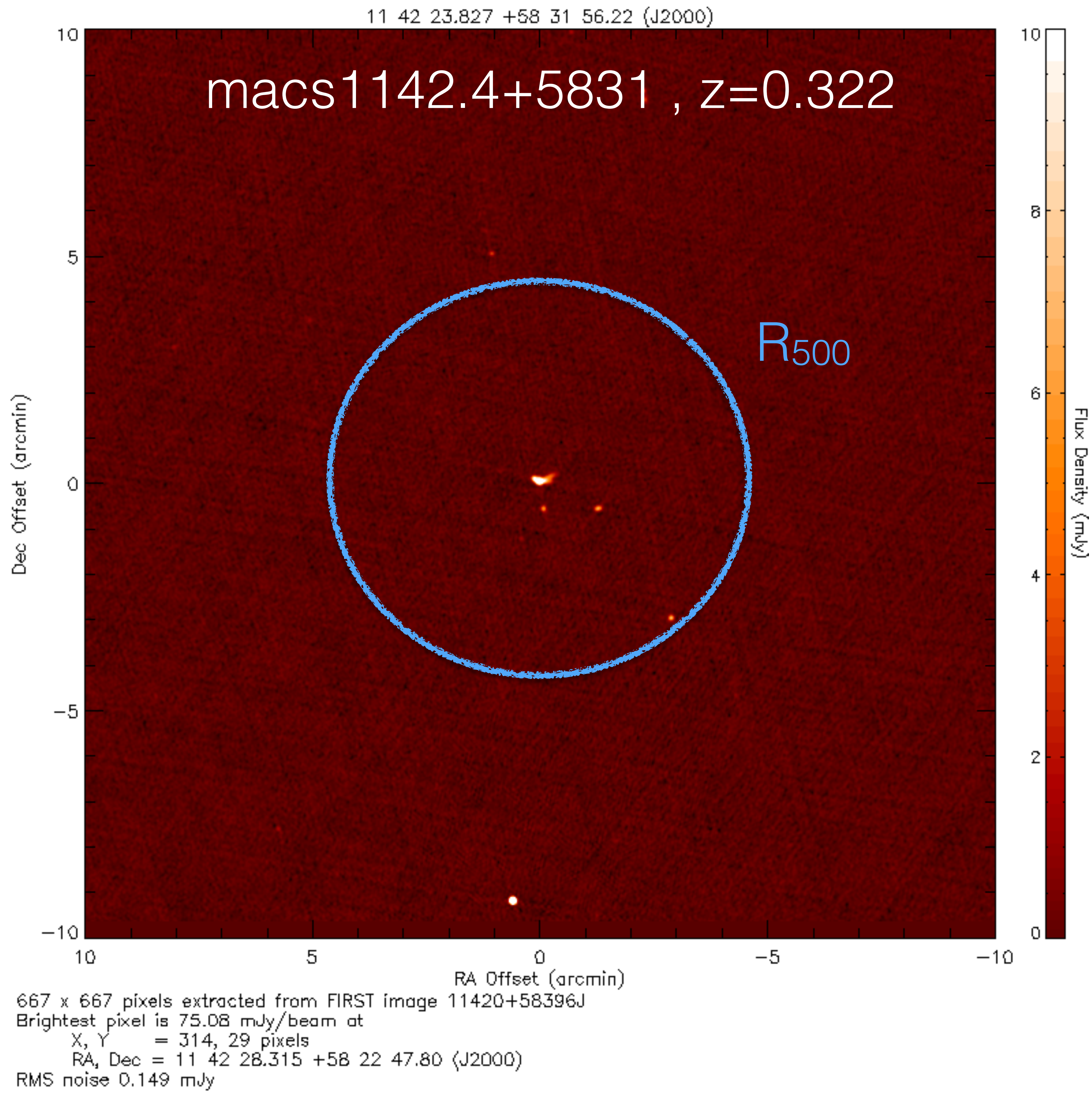
11 42 23.827 +58 31 56.22 (J2000)
macs1142.4+5831 , z=0.322
R500
Dec Offset (arcmin)
RA Offset (arcmin)
Flux Density (mJy)
10
5
0
−5
−10
8
6
4
2
667 x 667 pixels extracted from FIRST image 11420+58396J
Brightest pixel is 75.08 mJy/beam at
X, Y = 314, 29 pixels
RA, Dec = 11 42 28.315 +58 22 47.80 (J2000)
RMS noise 0.149 mJy

Redshift Evolution

$$\lambda(r) = \left(A_G \Phi_{RLF} \frac{1}{2\pi(\sigma^2+\epsilon^2)} e^{-\frac{r^2}{2(\sigma^2+\epsilon^2)}} + A_\beta \Phi_{RLF} \left(1+\left(\frac{r}{r_c}\right)^2\right)^{-3/2\beta+1/2} \right) \times D_A R_{500}(1+z)^3 + C_{Bkg}$$

Field RLF from Pracy et al. 2014

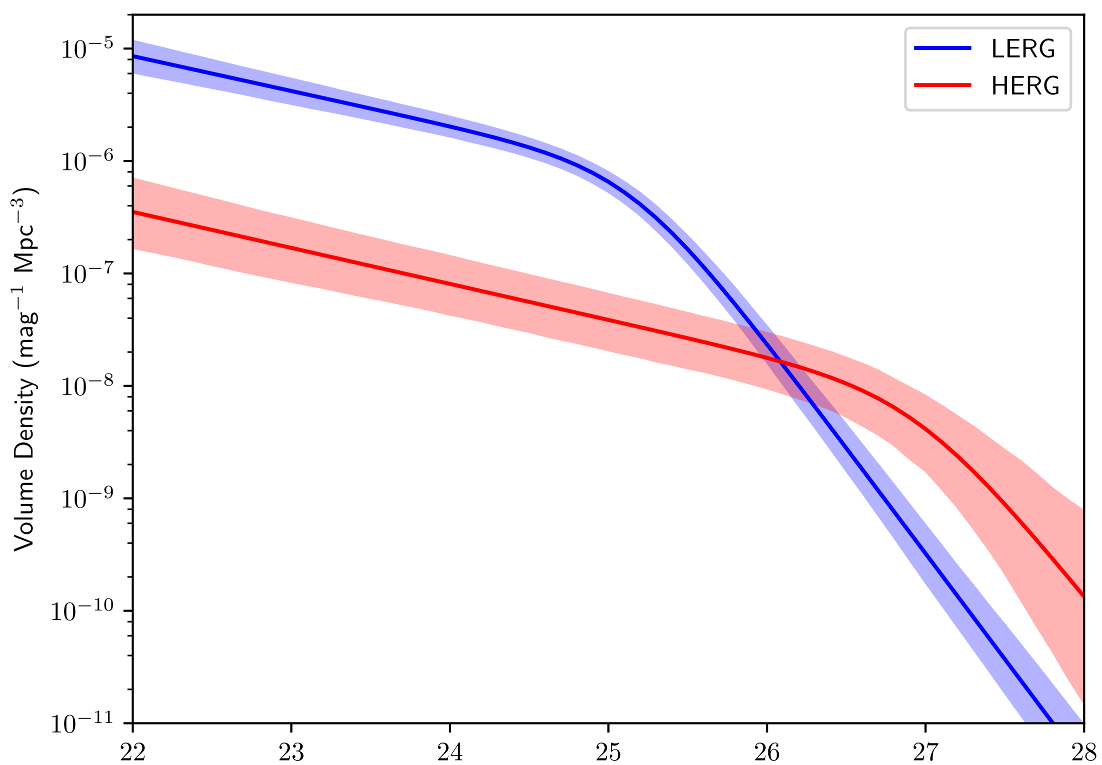

log L (W/Hz)

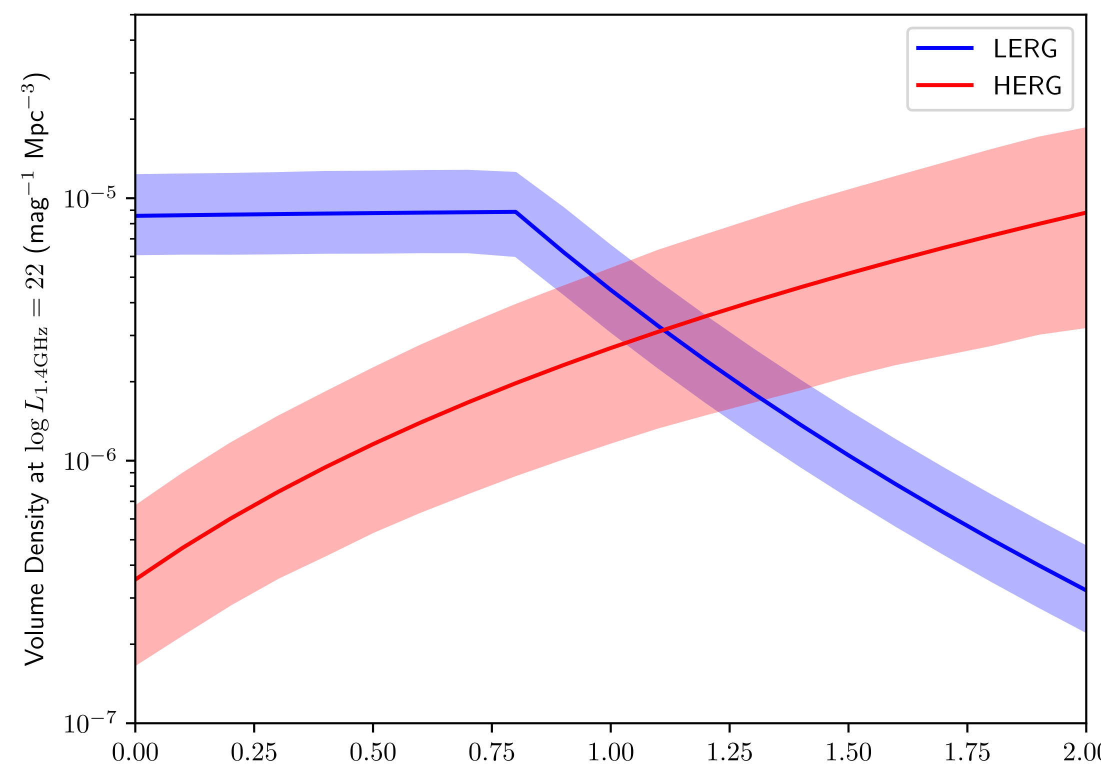

Redshift

Cluster number density is <u>consistent</u> with the field radio luminosity function redshift evolution

Cooling Flows

- Mittal et al. 2009
- Birzan et al. 2012

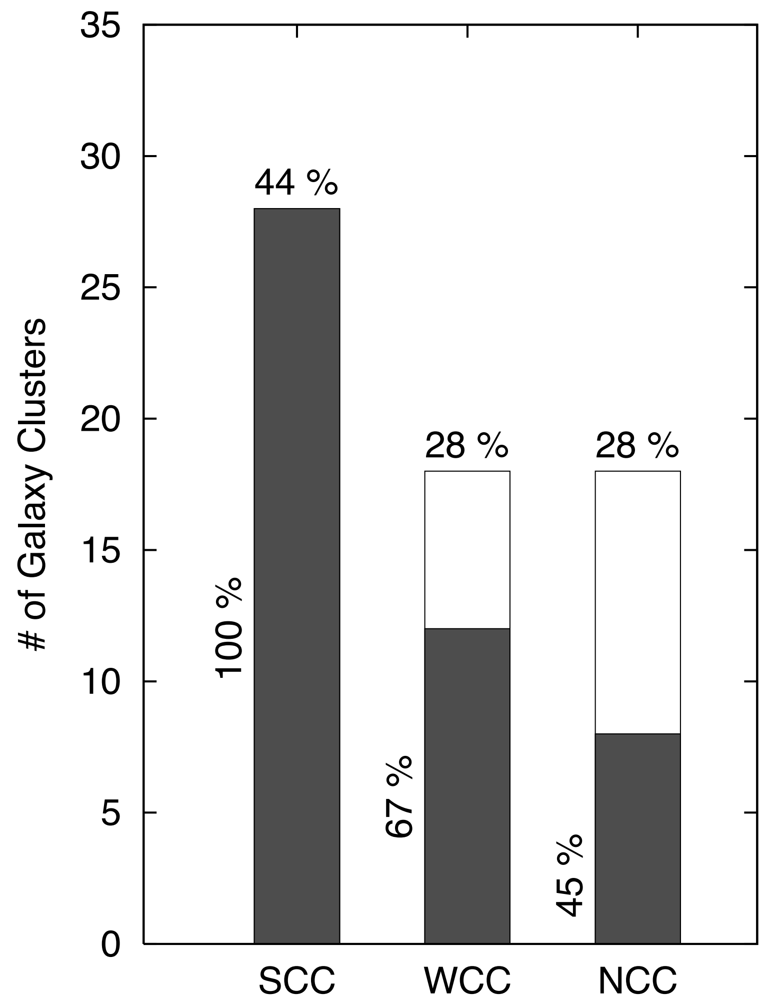

Fig. 6. The fraction of strong cool-core (SCC) clusters, weak cool-core (WCC) clusters and non-cool-core (NCC) clusters in the *HIFLUGCS* sample. Also shown are the fraction of clusters containing central radio sources for each category (shaded).

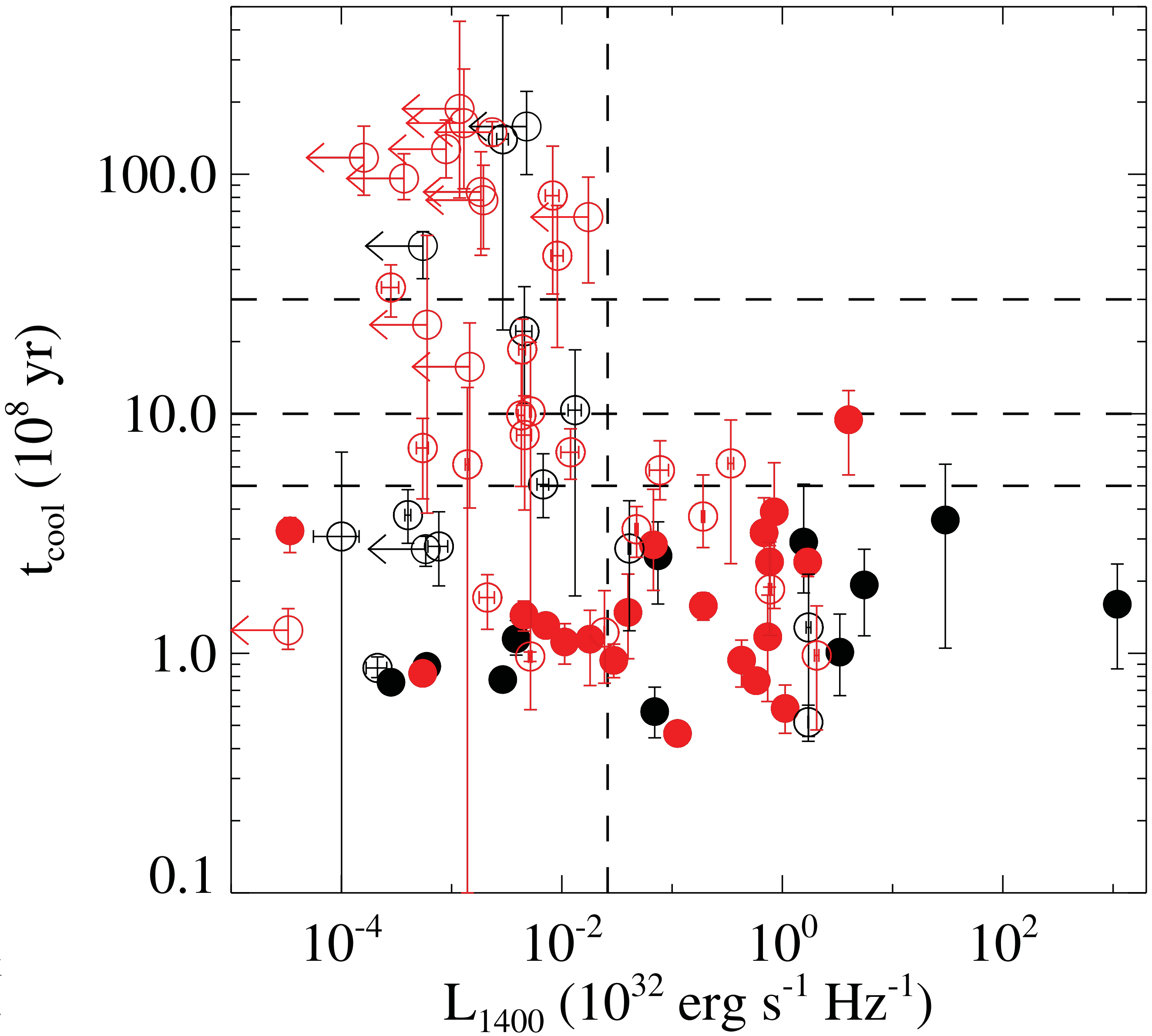

Redshift Evolution

$$\lambda(r) = \left(A_G \Phi_{RLF} \frac{1}{2\pi(\sigma^2+\epsilon^2)} e^{-\frac{r^2}{2(\sigma^2+\epsilon^2)}} + A_\beta \Phi_{RLF} \left(1 + \left(\frac{r}{r_c}\right)^2\right)^{-3/2\beta+1/2} \right) \times D_A R_{500} (1+z)^3 + C_{Bkg}$$

$$\Phi_{RLF} = \Phi_{LERG} + \Phi_{HERG}$$

$$\Phi_i = \int_{L_{limit}}^{\infty} \frac{C_i}{(L_i^* e_i(z)/L)^{\gamma_{1,i}} + (L_i^* e_i(z)/L)^{\gamma_{2,i}}} dL$$

Pure Luminosity Evolution

$$e_{j,i}(\mathrm{z}) \begin{cases} (1+z)^{p_{1,i}+\alpha_{z,j}} & : z \leq z_{c,i} \\ (1+z_{c,i})^{p_{1,i}+\alpha_{z,j}} \left(\frac{1+z}{1+z_{c,i}}\right)^{p_{2,i}} & : z > z_{c,i}. \end{cases}$$

X-ray AGN evolution

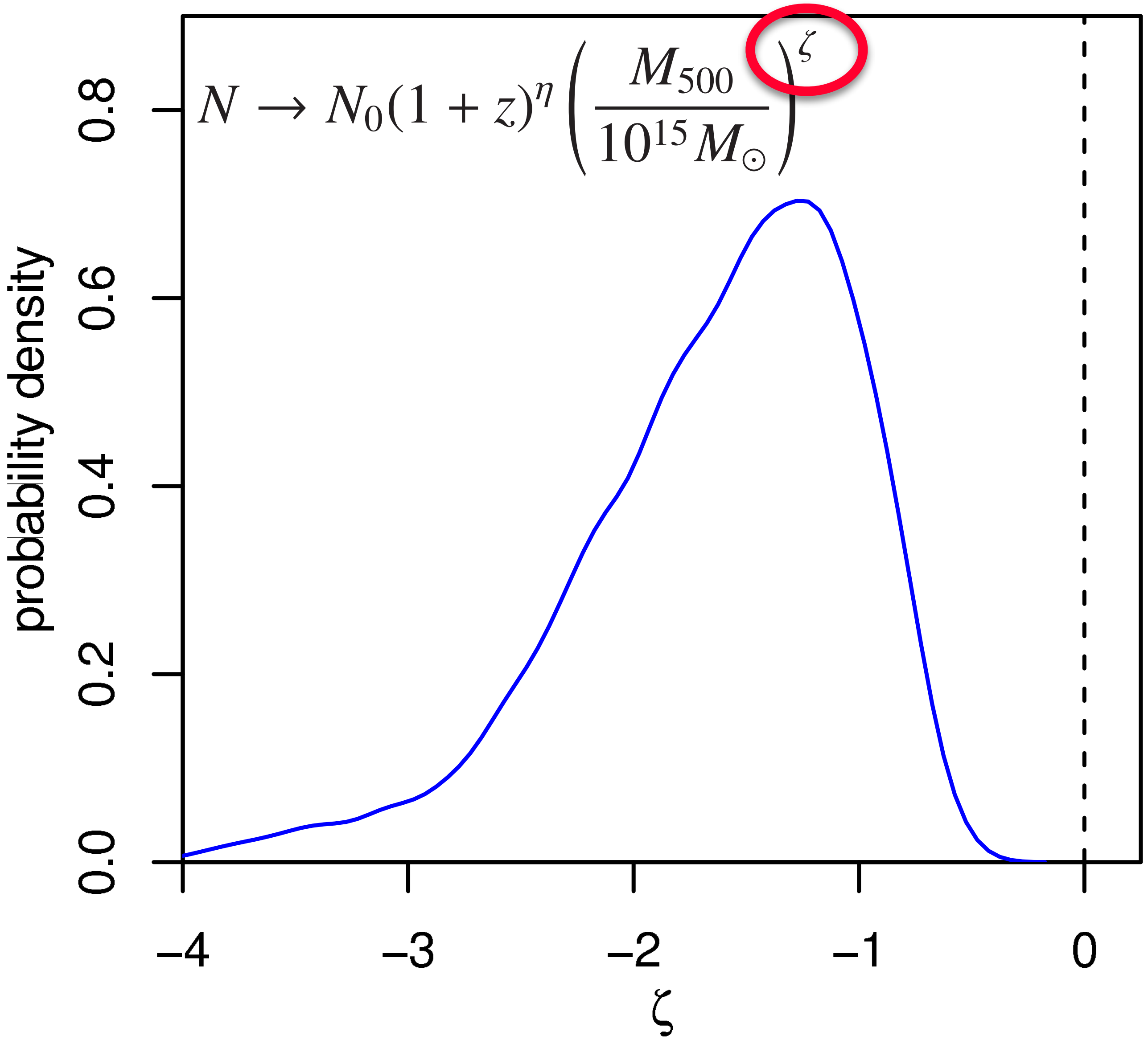

Mass dependence of scale factor

ζ ~ -1.2

Scale factor has a $M^{-1.2}$ dependence

ζ = 0 rejected at >99.9%

No other parameters are significantly different from zero

Ehlert et al. 2015

Radio AGN Model

$$\lambda(r) = \left(A_G \Phi_{RLF} \frac{1}{2\pi(\sigma^2+\epsilon^2)} e^{-\frac{r^2}{2(\sigma^2+\epsilon^2)}} + A_\beta \Phi_{RLF} \left(1+\left(\frac{r}{r_c}\right)^2\right)^{-3/2\beta+1/2} \right) \times D_A R_{500} (1+z)^3 + C_{Bkg}$$

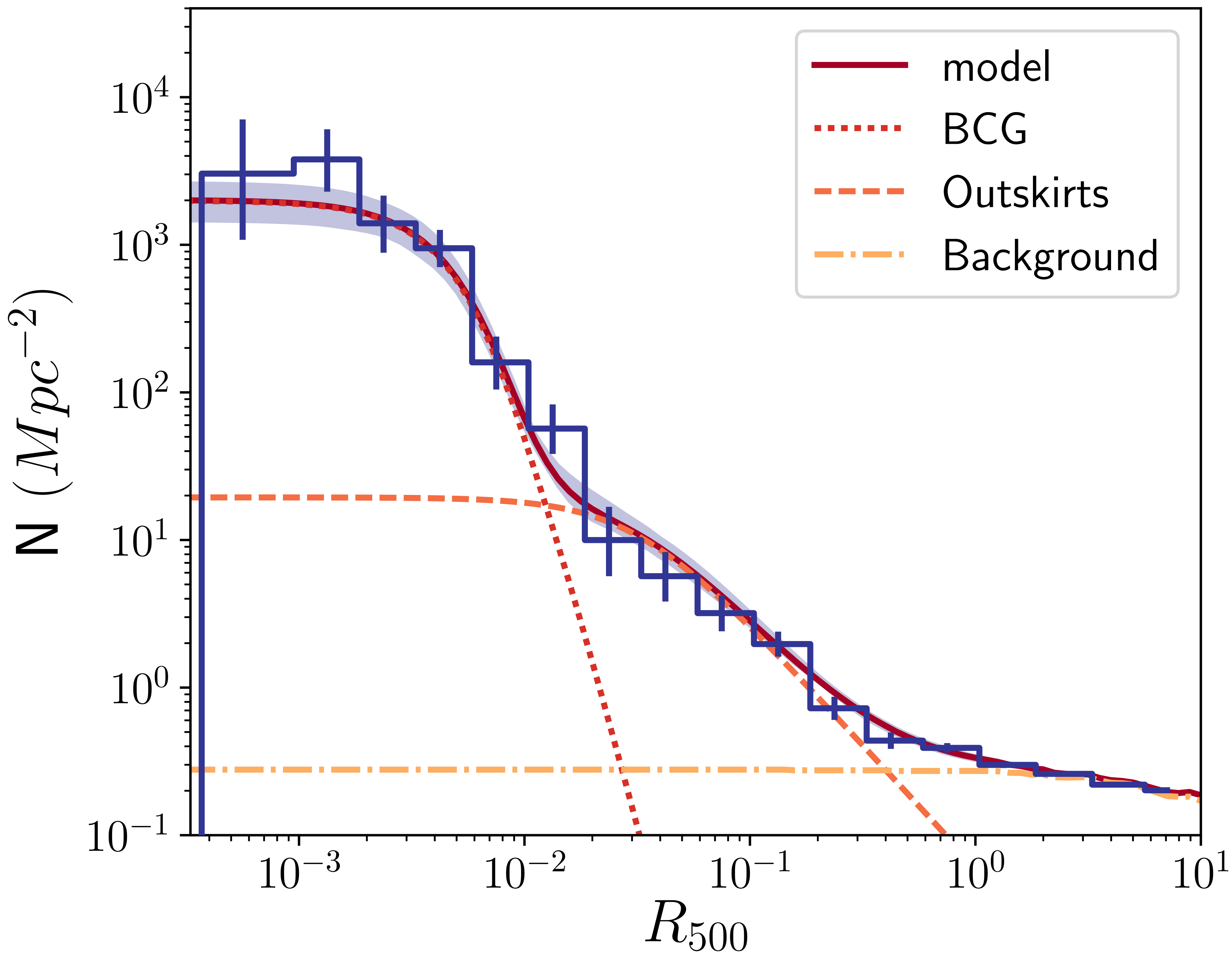

Mergers & Tidal Interactions

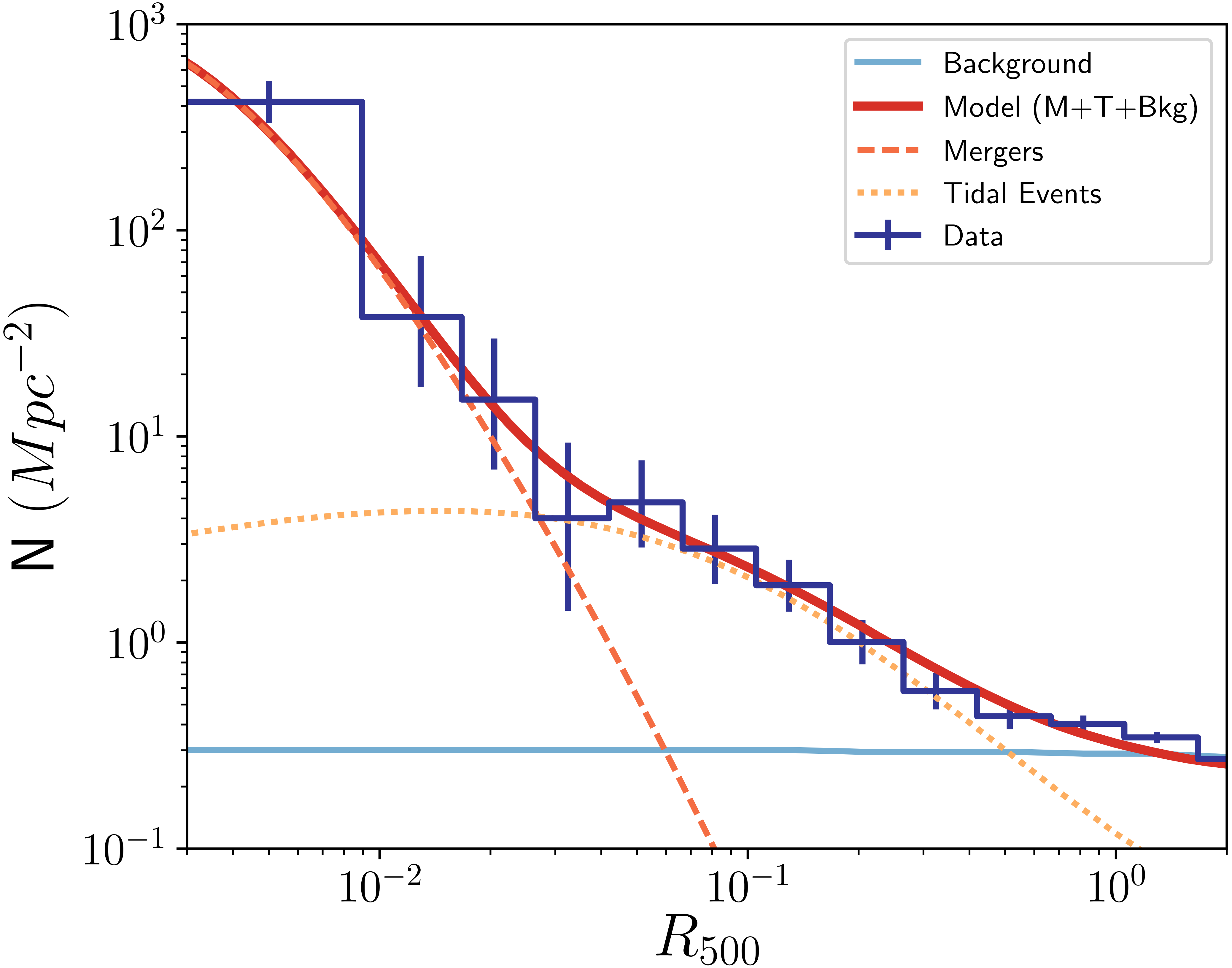

Flux & Luminosity Limits

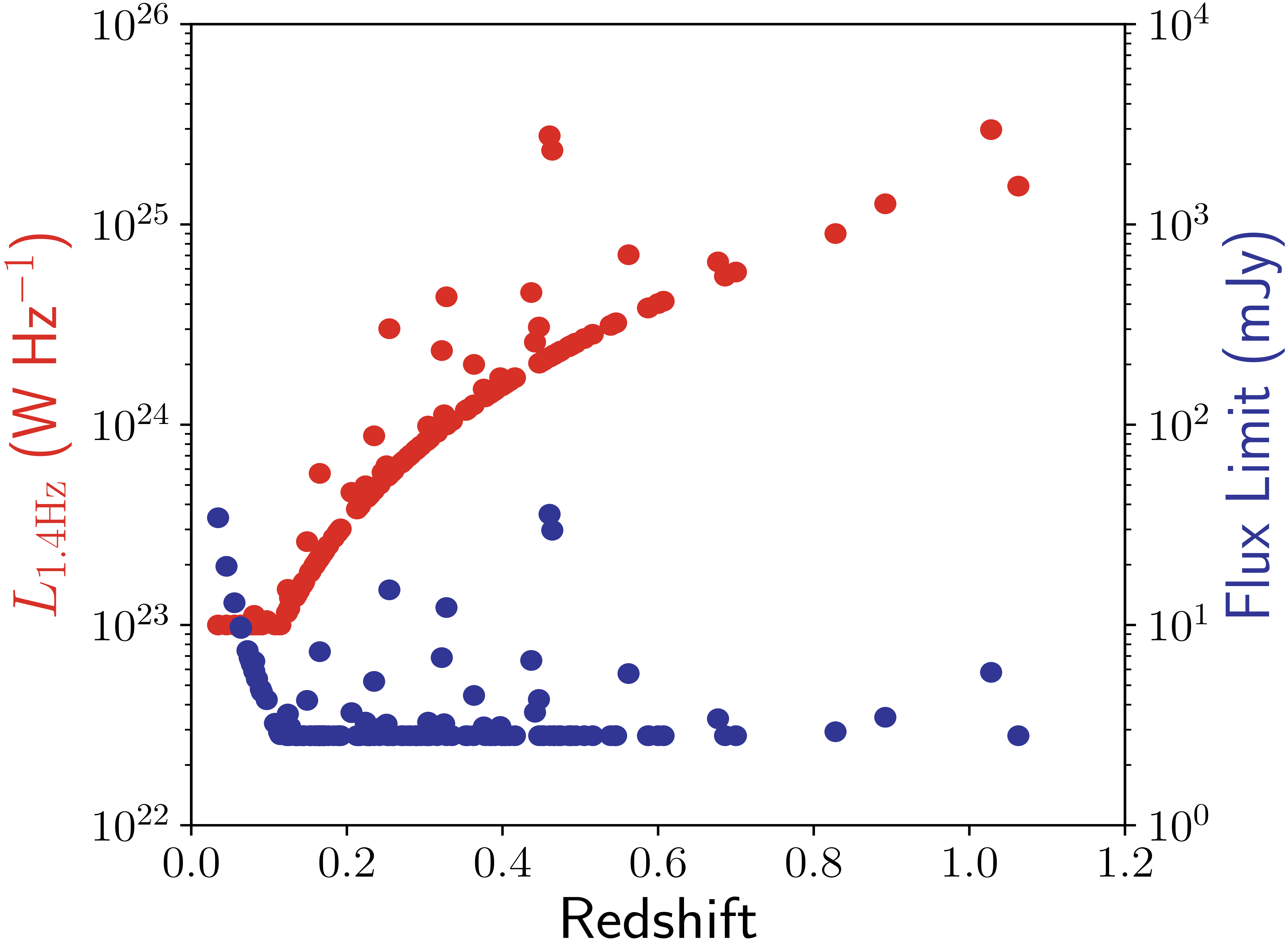

Radio Cluster AGN

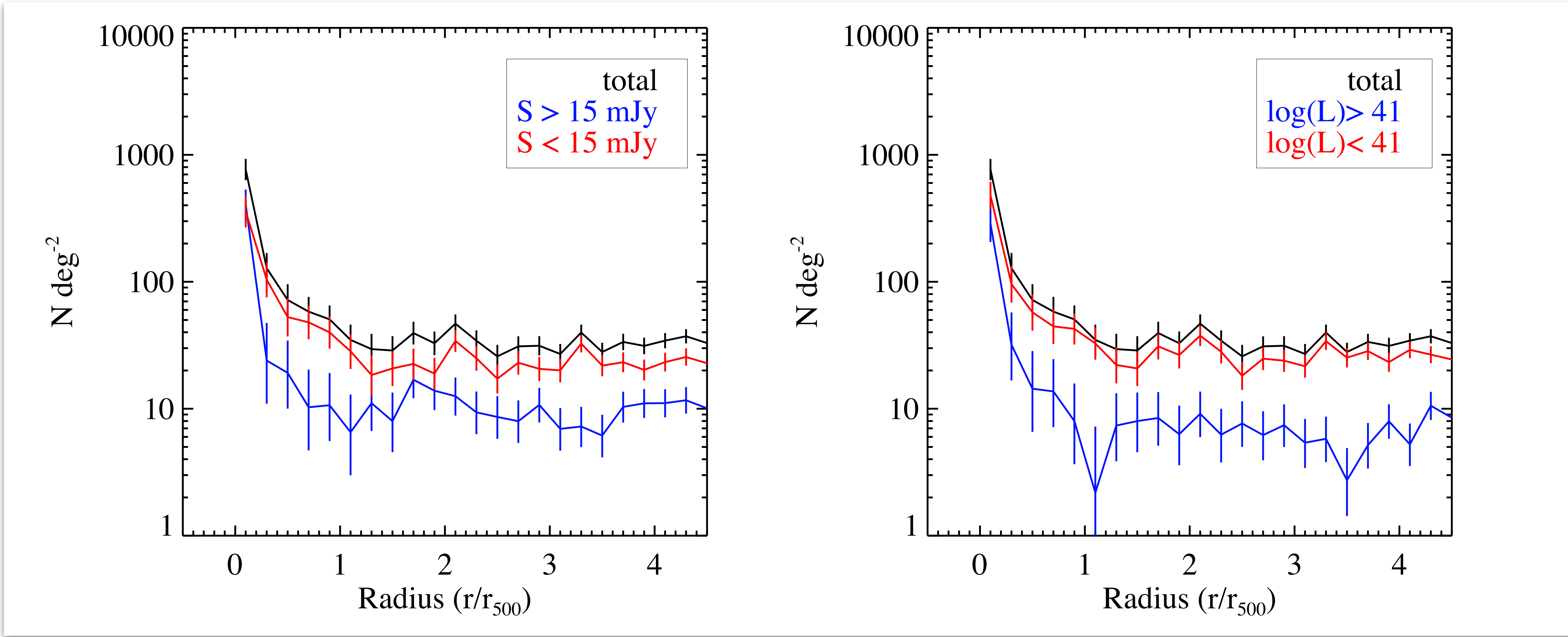

- Both high and low luminosity sources increase in number density at the center

- Log L= 41 is roughly the divide between FR I and FR II sources

Radio Cluster AGN

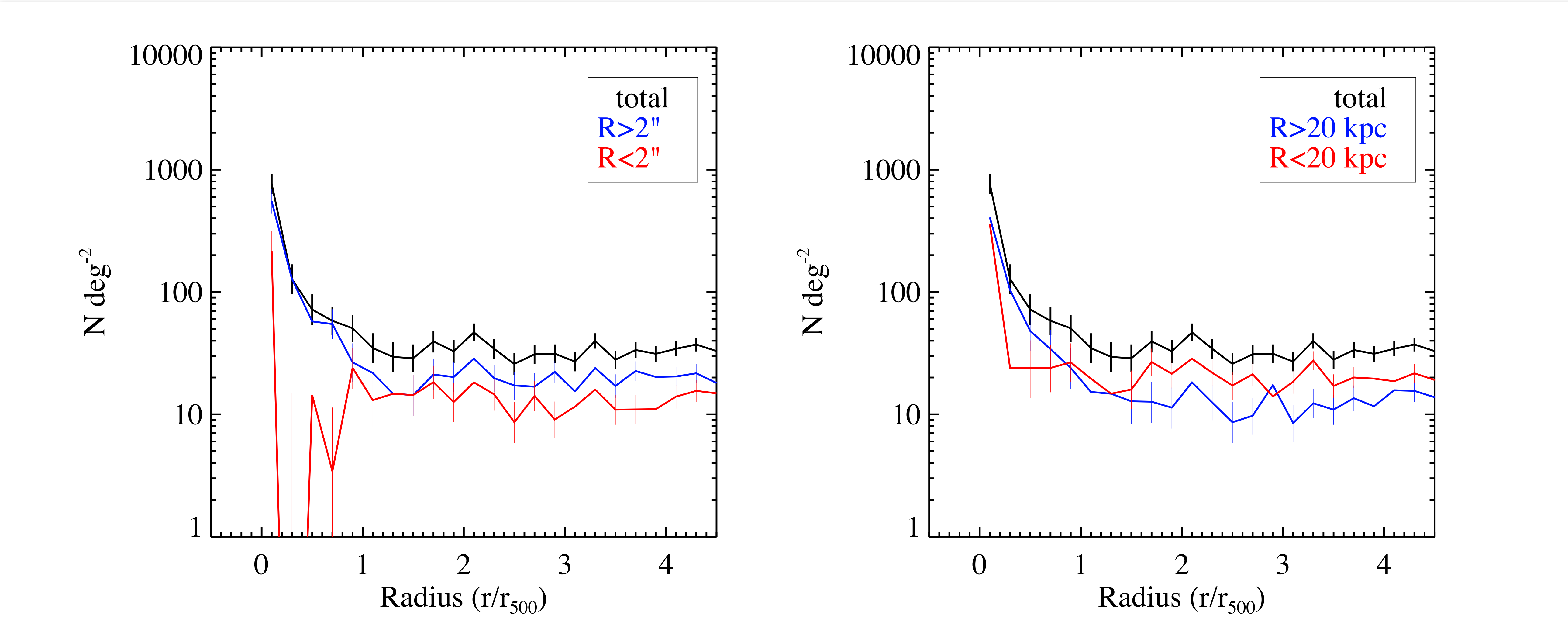

- Extended sources preferentially increase inside clusters
- Gas pressure increases in clusters, which could confine extended sources but we observe the opposite.

Motivation

- Jet power measured from pdV work need to inflate cavities scales with 1.4 GHz radio luminosities
  - giant Ellipticals
  - Cavagnolo et al. 2010

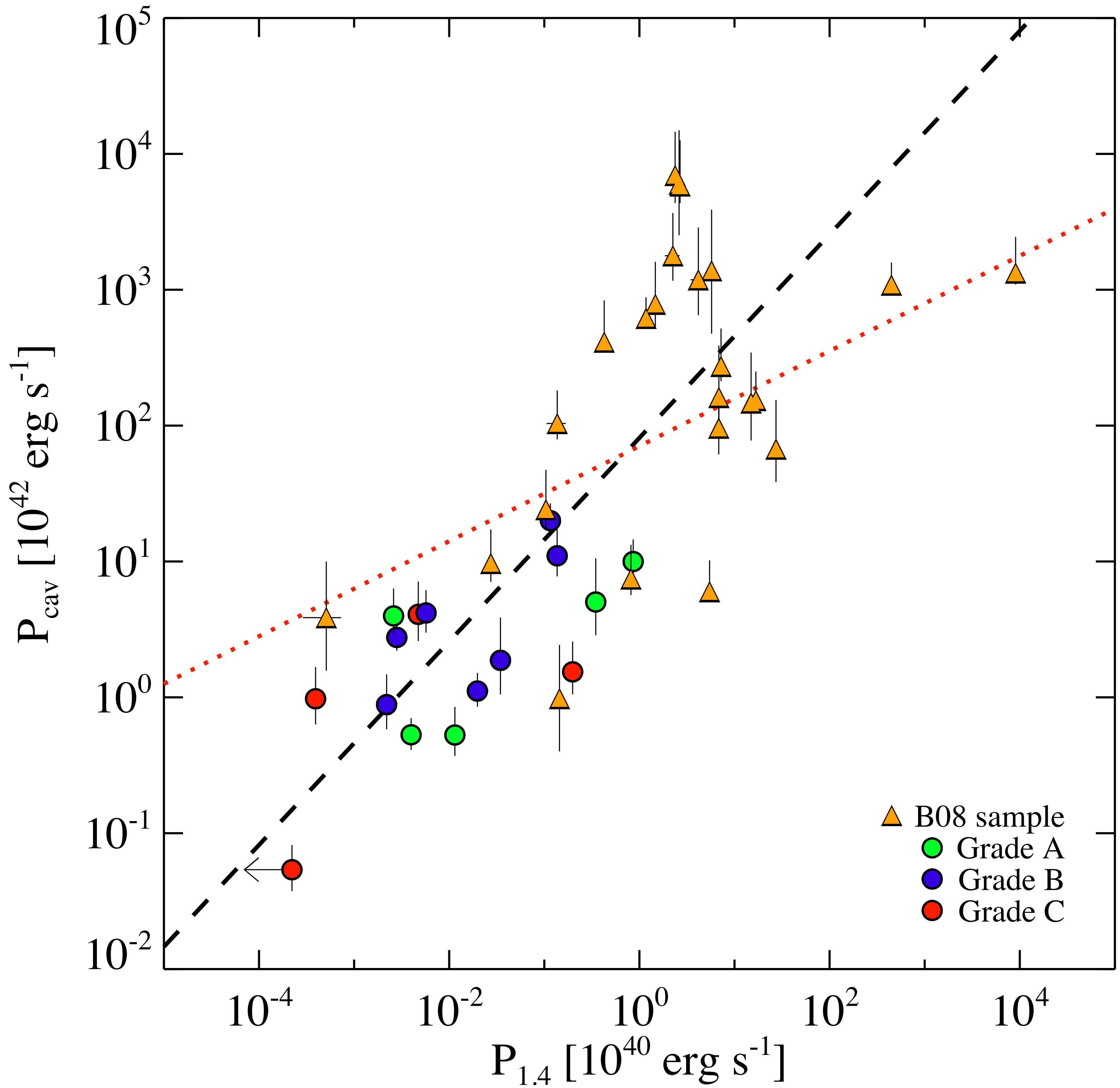

Cooling Flows

- Mittal et al. 2009

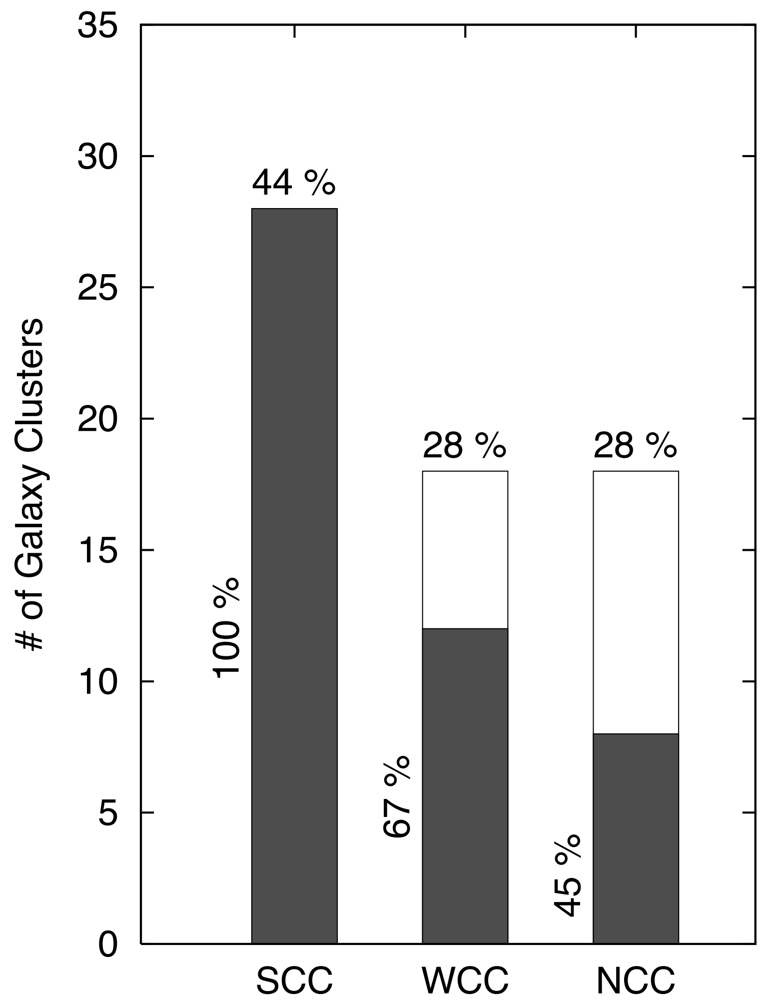

Fig. 6. The fraction of strong cool-core (SCC) clusters, weak cool-core (WCC) clusters and non-cool-core (NCC) clusters in the *HIFLUGCS* sample. Also shown are the fraction of clusters containing central radio sources for each category (shaded).

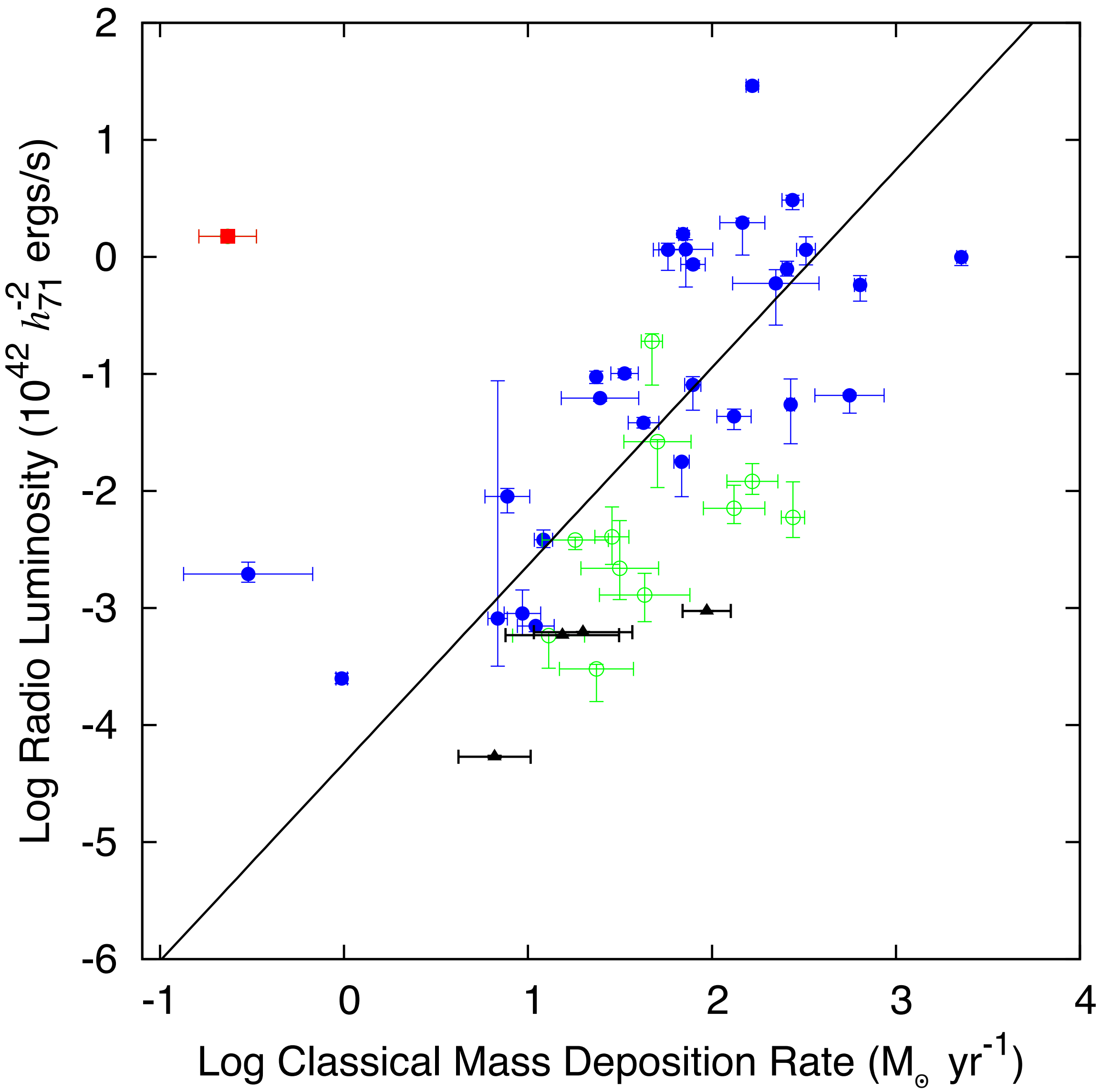

Relaxed Clusters and Cooling Flows

- Relaxation timescales

$$t_{relax} \simeq \frac{R}{v}\frac{N}{\ln N}$$

$$N \propto M$$

$$t_{relax} \propto \frac{M}{\ln M}$$

- Cooling timescales

$$t_{cool} \propto \frac{T}{n\Lambda(T)}$$

$$M \propto T^{3/2}$$

$$t_{cool} \underset{\sim}{\propto} M^{2/3}$$

X-ray AGN evolution

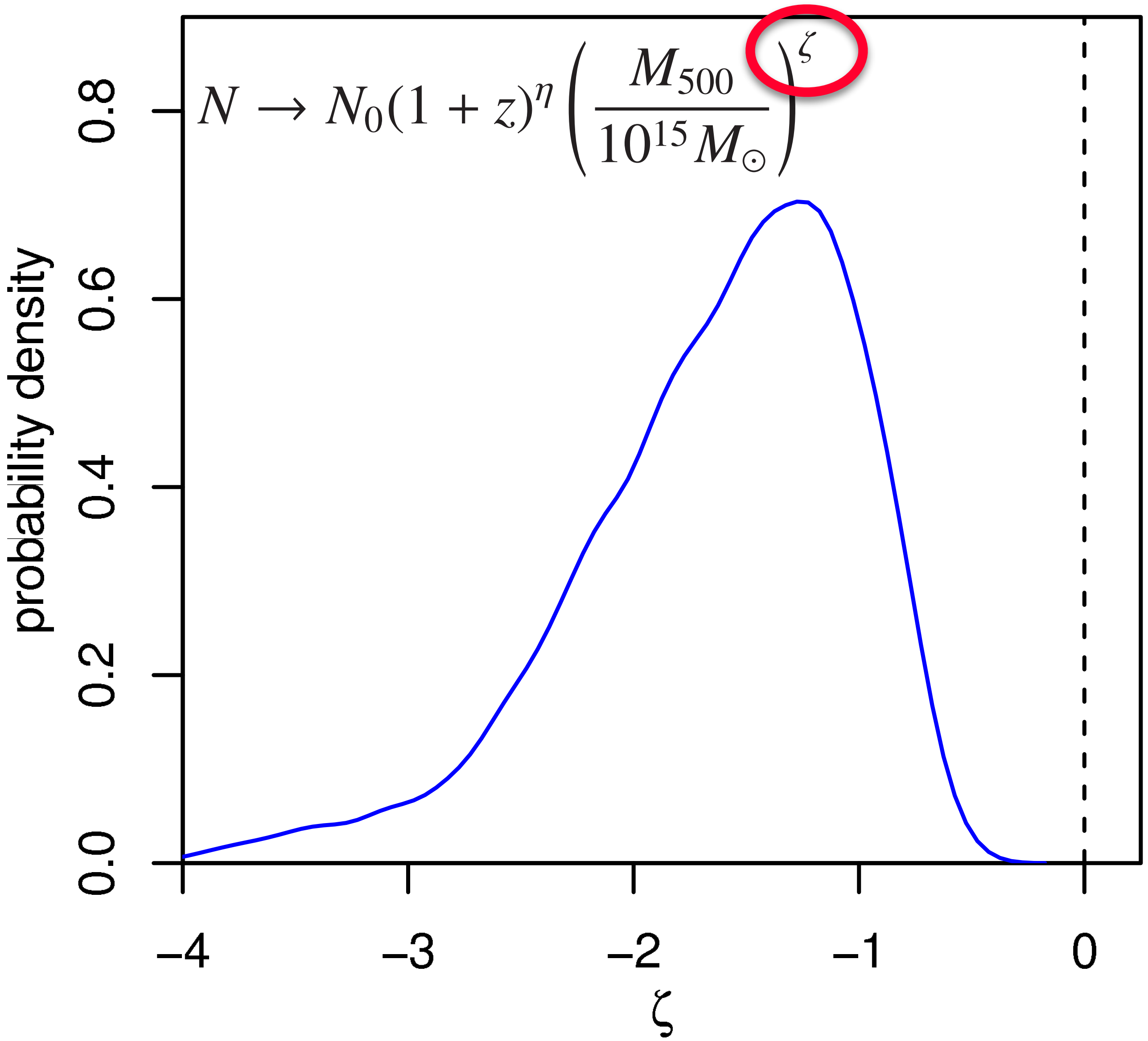

Mass dependence of scale factor

ζ ~ -1.2

Scale factor has a $M^{-1.2}$ dependence

ζ = 0 rejected at >99.9%

No other parameters are significantly different from zero

Consistent with Merger Triggering

Radio AGN Overdensity in Cluster Center (<1 R_{500})

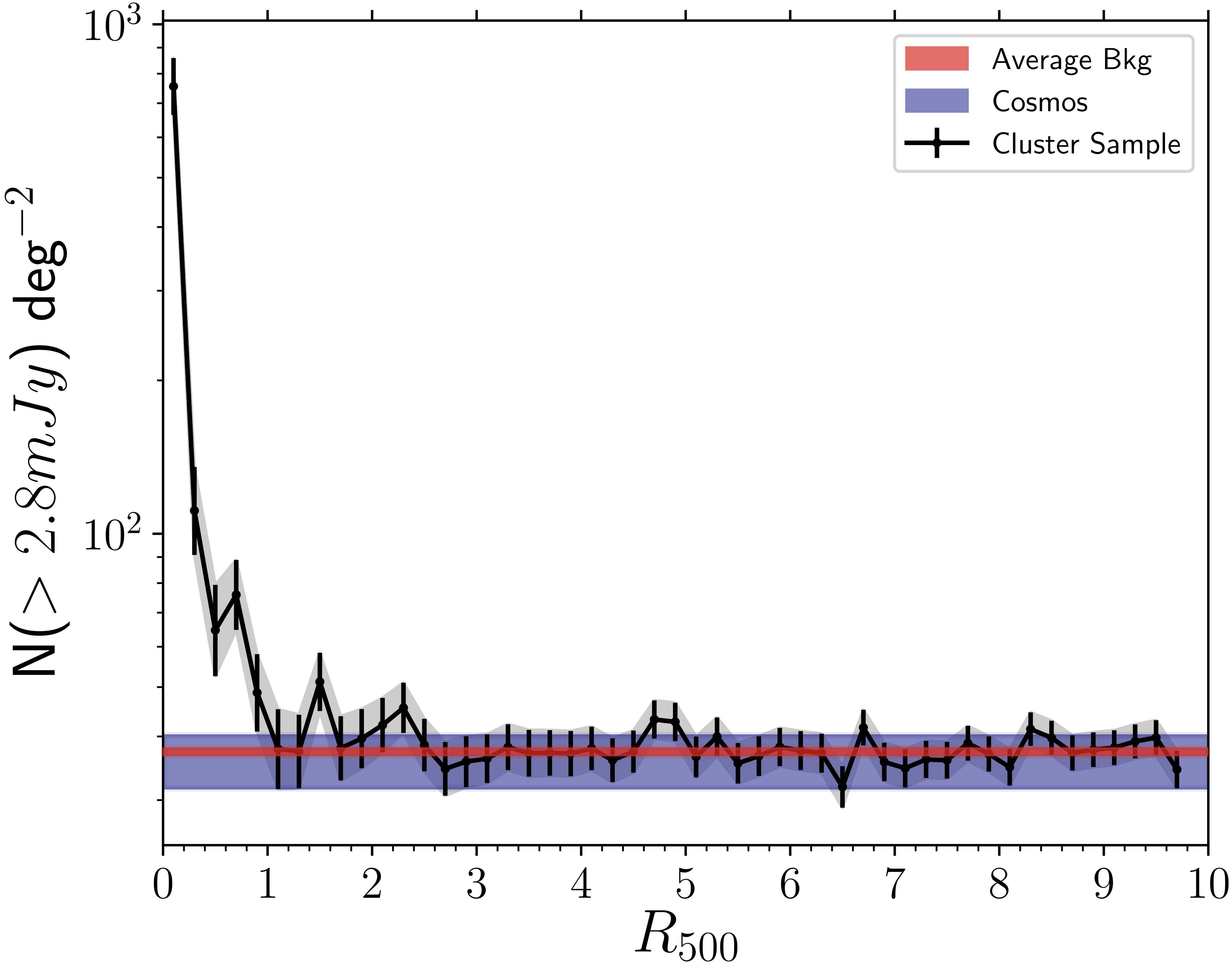

X-ray AGN Overdensity in Cluster Center (<2 R_{500})

Elhert et al. 2014

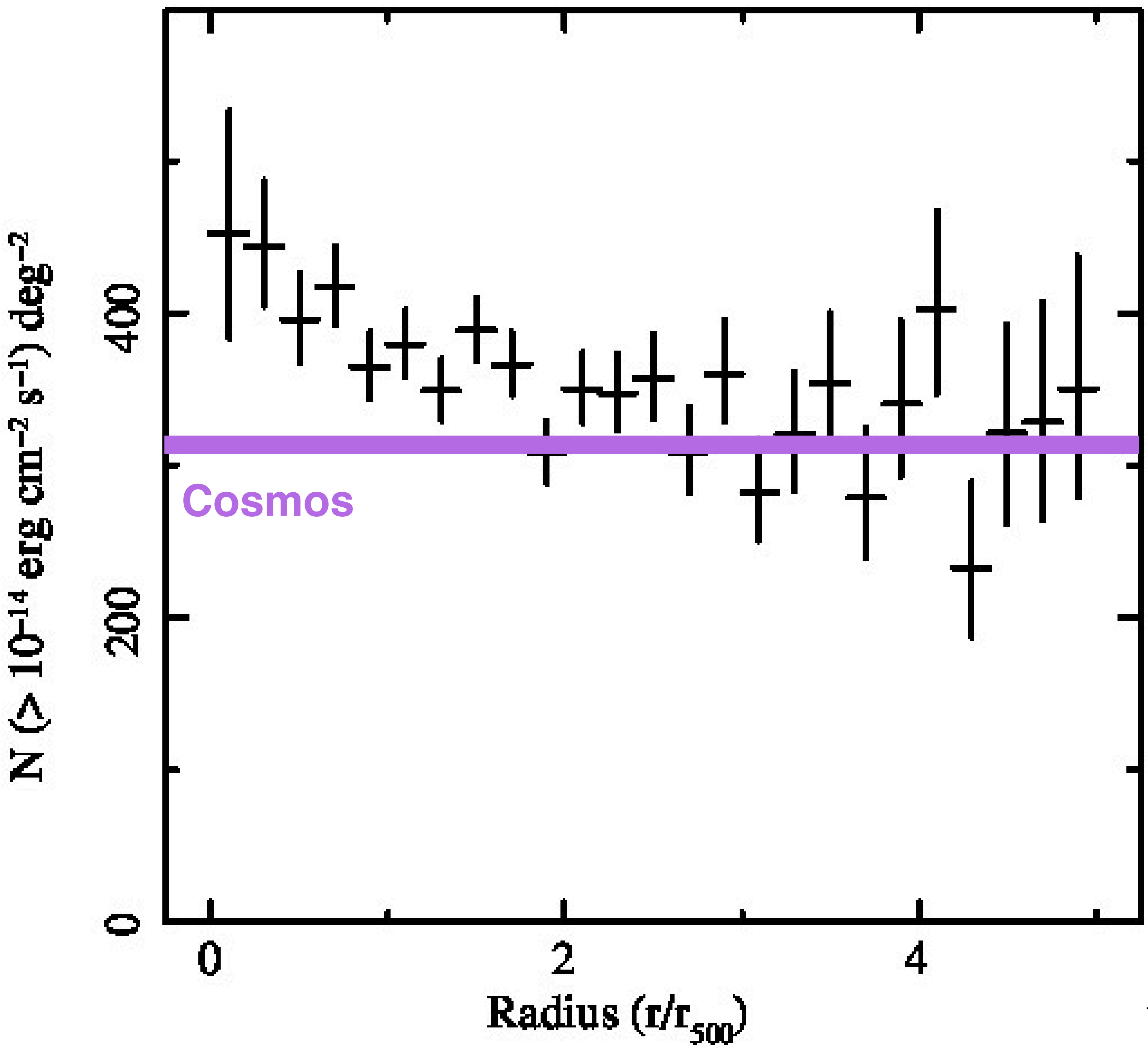

Active Cluster AGN Fraction

X-ray/Optical

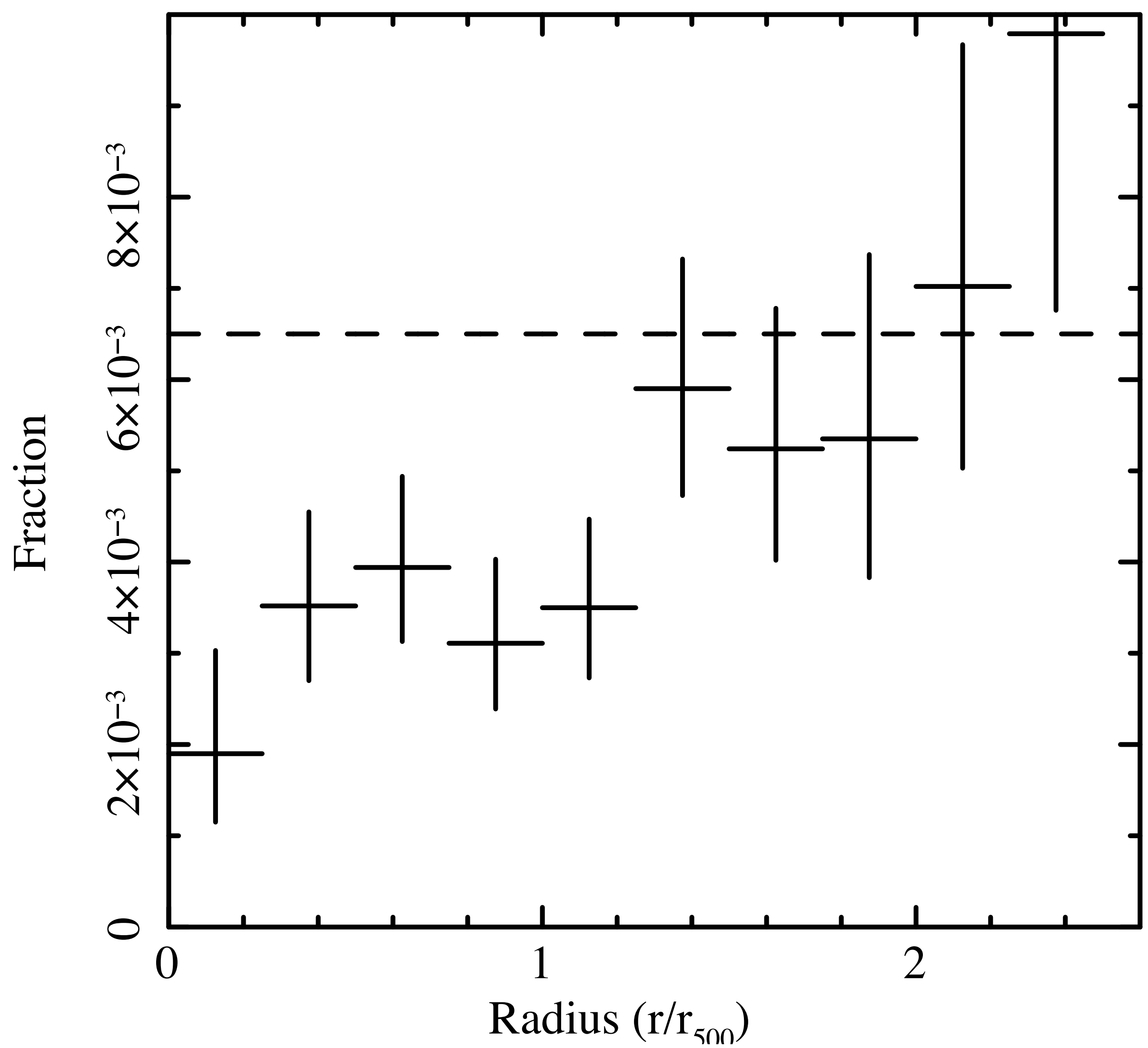

Radiative Mode

Radio/Optical

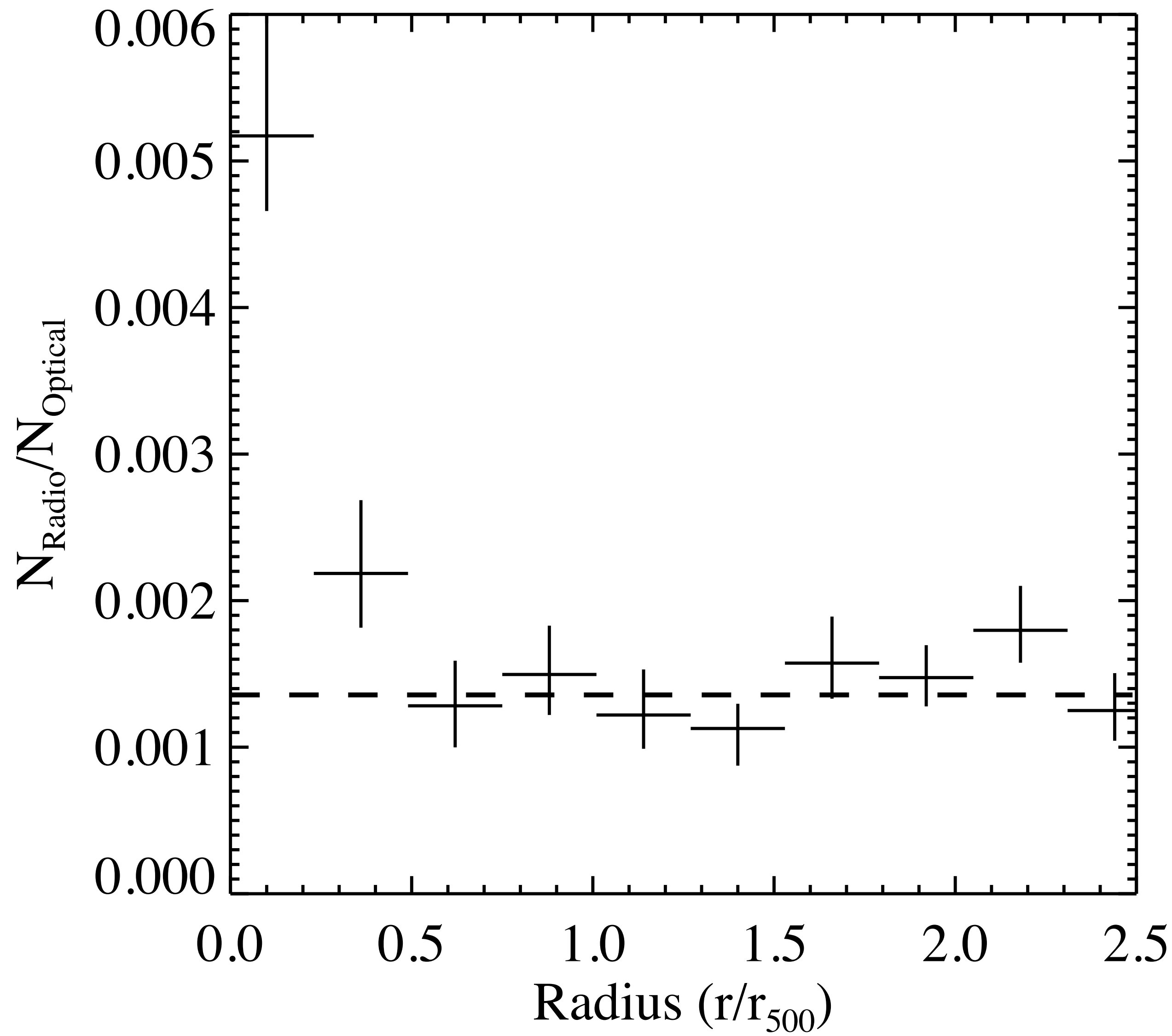

Kinetic Mode

Low Mass Accretion Rates

- Radio emission is sensitive to:
    - low Eddington Accretion
        - may be more efficient at creating jets -> ADAF/Thick Disks
    - Hot Mode Accretion
        - Cold Gas is stripped from the galaxies
        - could also result in an extended disk
    - Massive Black Holes

Mass or redshift evolution?

$$N_{\mathrm{obs}}(> f, r, z) = N \times D_{\mathrm{A}}(z)^2 \times r_{500} \times \Phi(> L_{\mathrm{cut}}, z) \times \left(\frac{r}{r_{500}}\right)^{\beta} + C$$

Projected number density of observed X-ray AGN in a cluster field at a given cluster z, r and above flux limit f = **Projected number density of X-ray AGN expected in cluster** above flux limit + **Projected number density of all field AGN** above flux limit

'Scale factor' which allows number density to exceed co-moving field AGN X Scaled by radius X Co-moving field AGN number density at z and above luminosity related to flux limit X Some radial dependence

Allow a mass and redshift dependence for scale factor (normalisation) and radial scaling

$$N \to N_0(1+z)^{\eta}\left(\frac{M_{500}}{10^{15}M_{\odot}}\right)^{\zeta} \qquad \beta \to \beta_0 + \beta_{\mathrm{z}}(1+z) + \beta_{\mathrm{m}}\left(\frac{M_{500}}{10^{15}M_{\odot}}\right)$$

Radio AGN Evolution

- Pracy et al. 2014
- 1.4 GHz radio luminosity
    - Low-Excitation Radio Galaxies
    - High-Excitation Radio Galaxies
- LERG and HERG have separate evolutions
    - LERG are relatively constant to z~1
    - HERG evolve more like Quasars

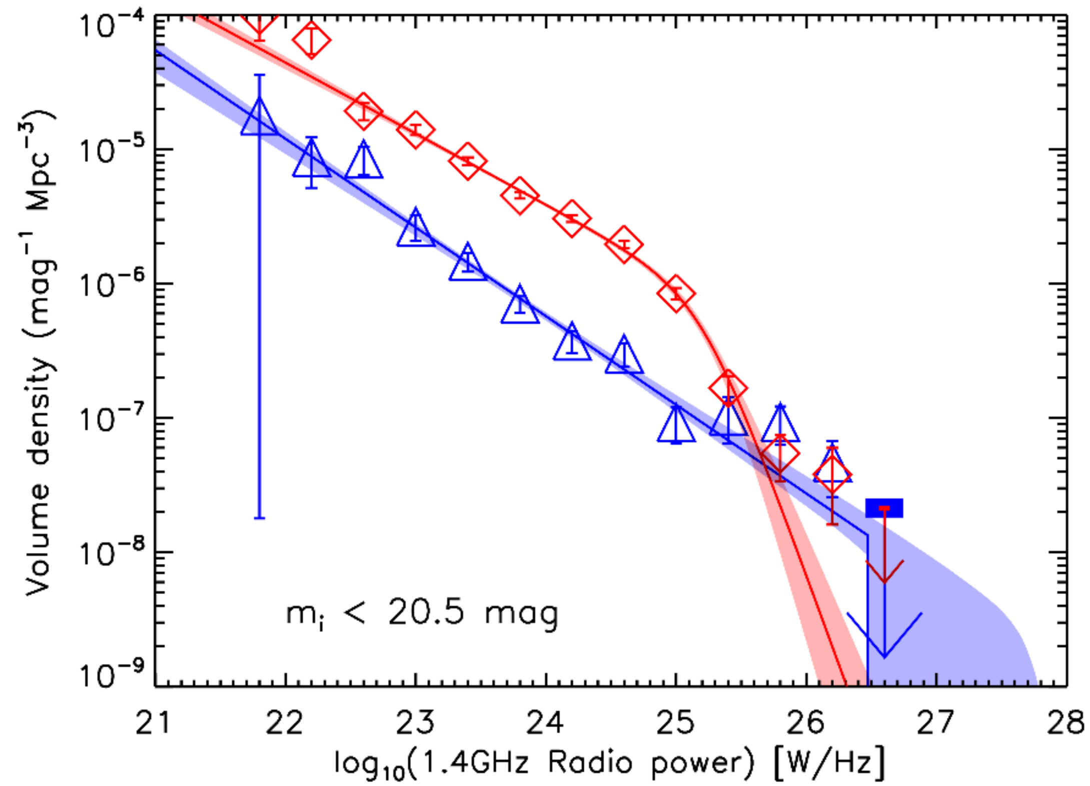

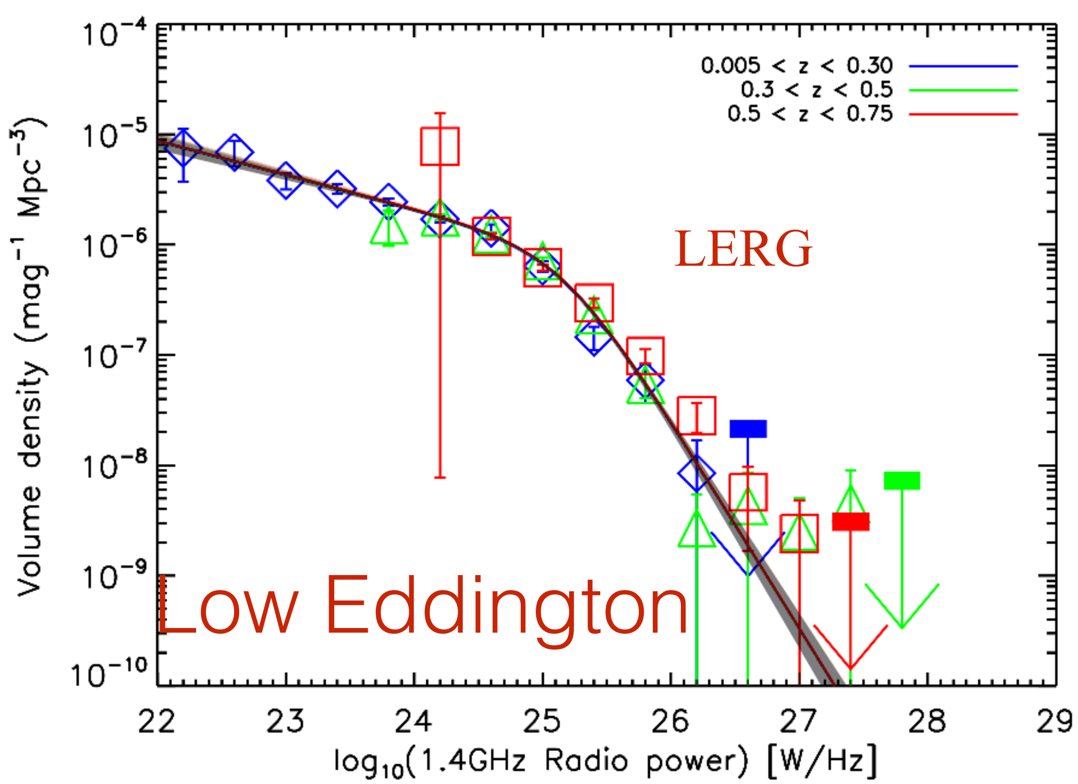

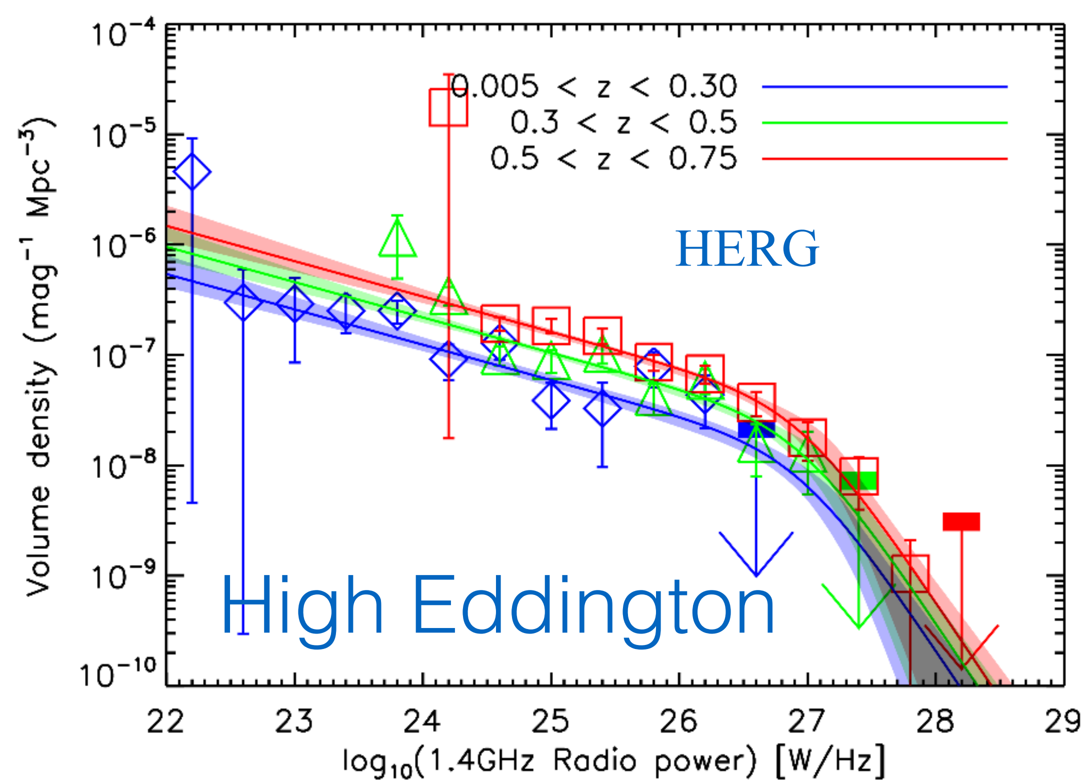

Spectroscopic Follow-up

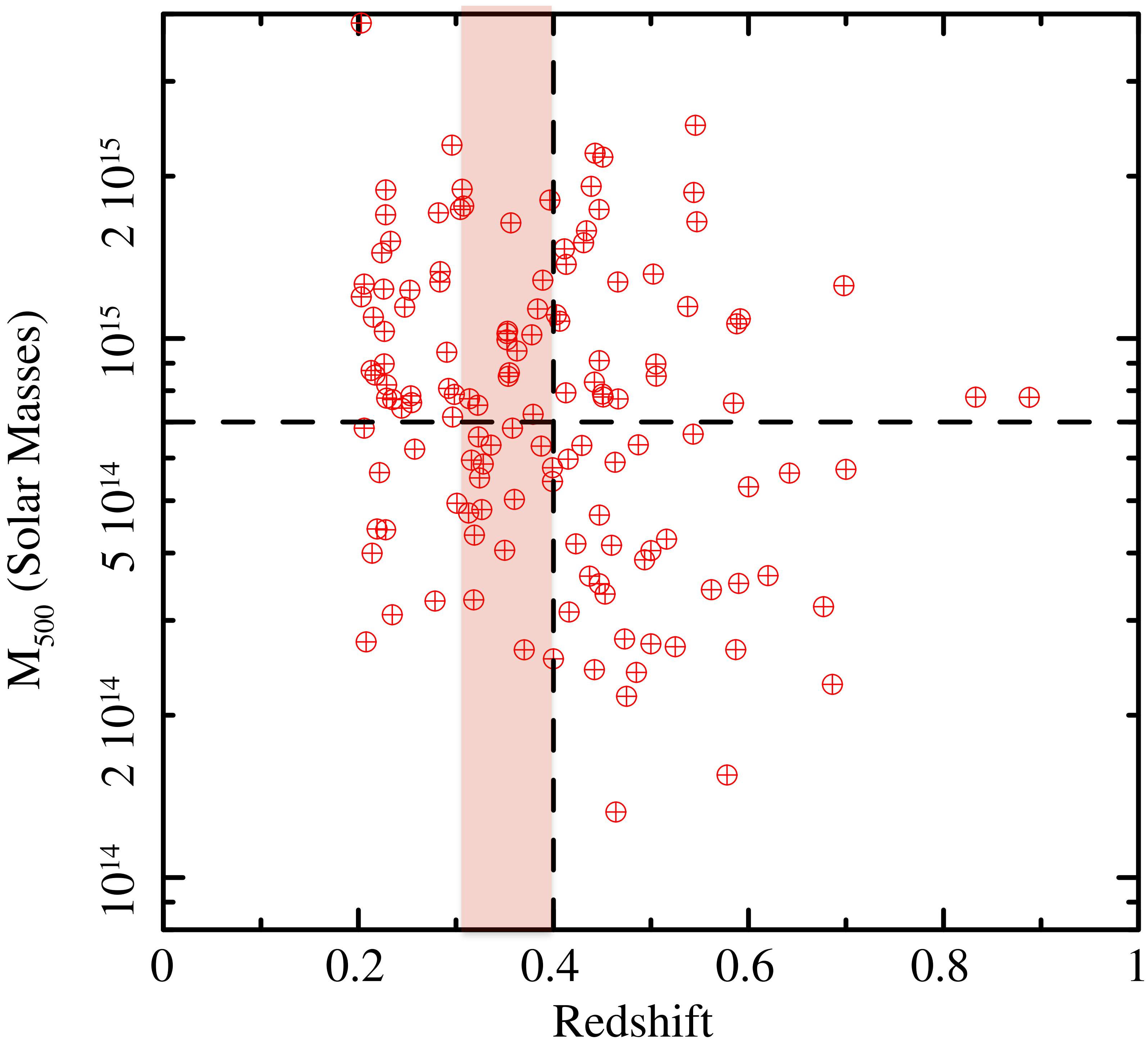

VIMOS follow-up program:

Observe 10, z=0.35 - 0.4, relaxed clusters

Aims:
- Examine X-ray AGN host relationship
- Does AGN fraction depend on cluster mass?

Mass and Redshift

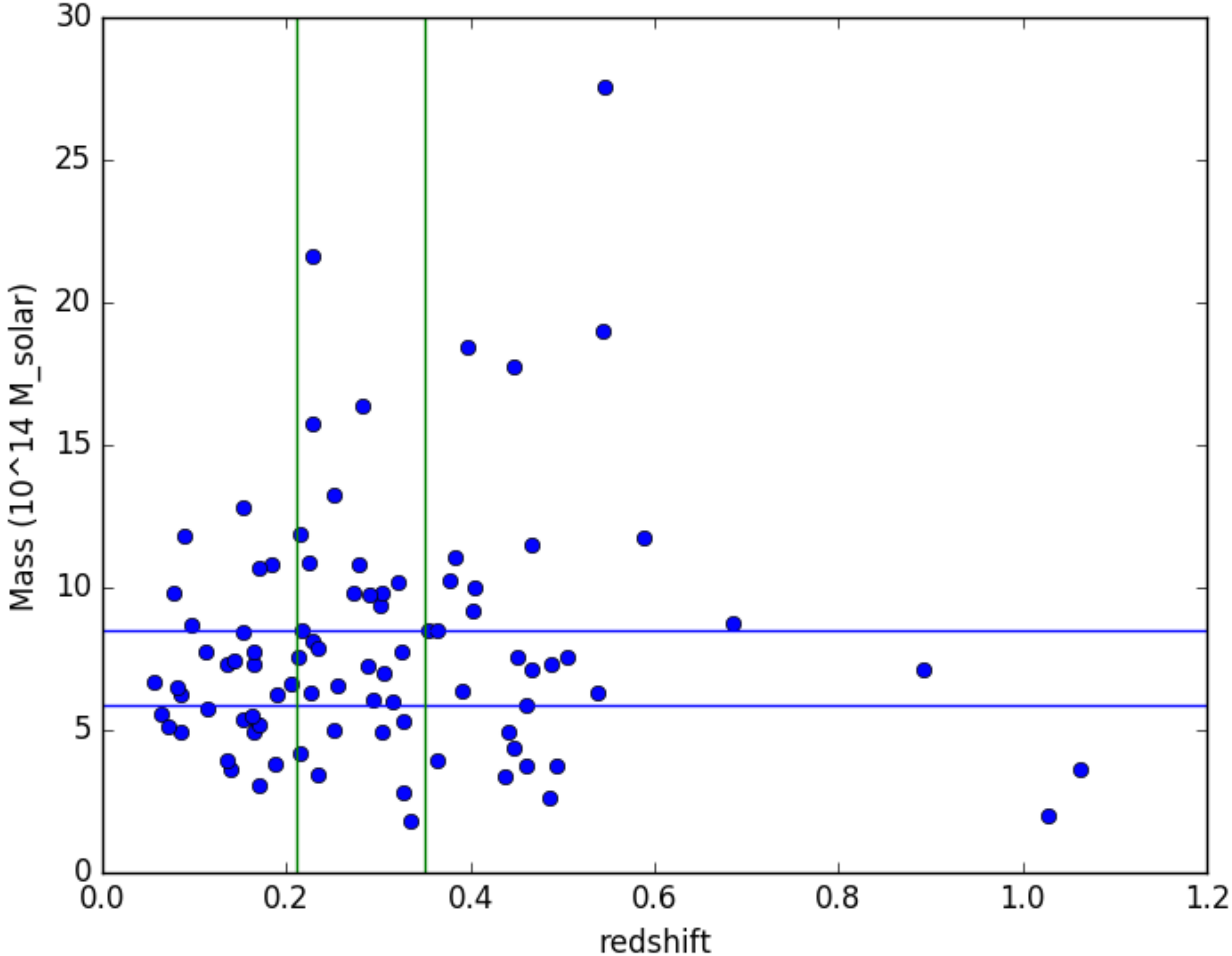

Feedback

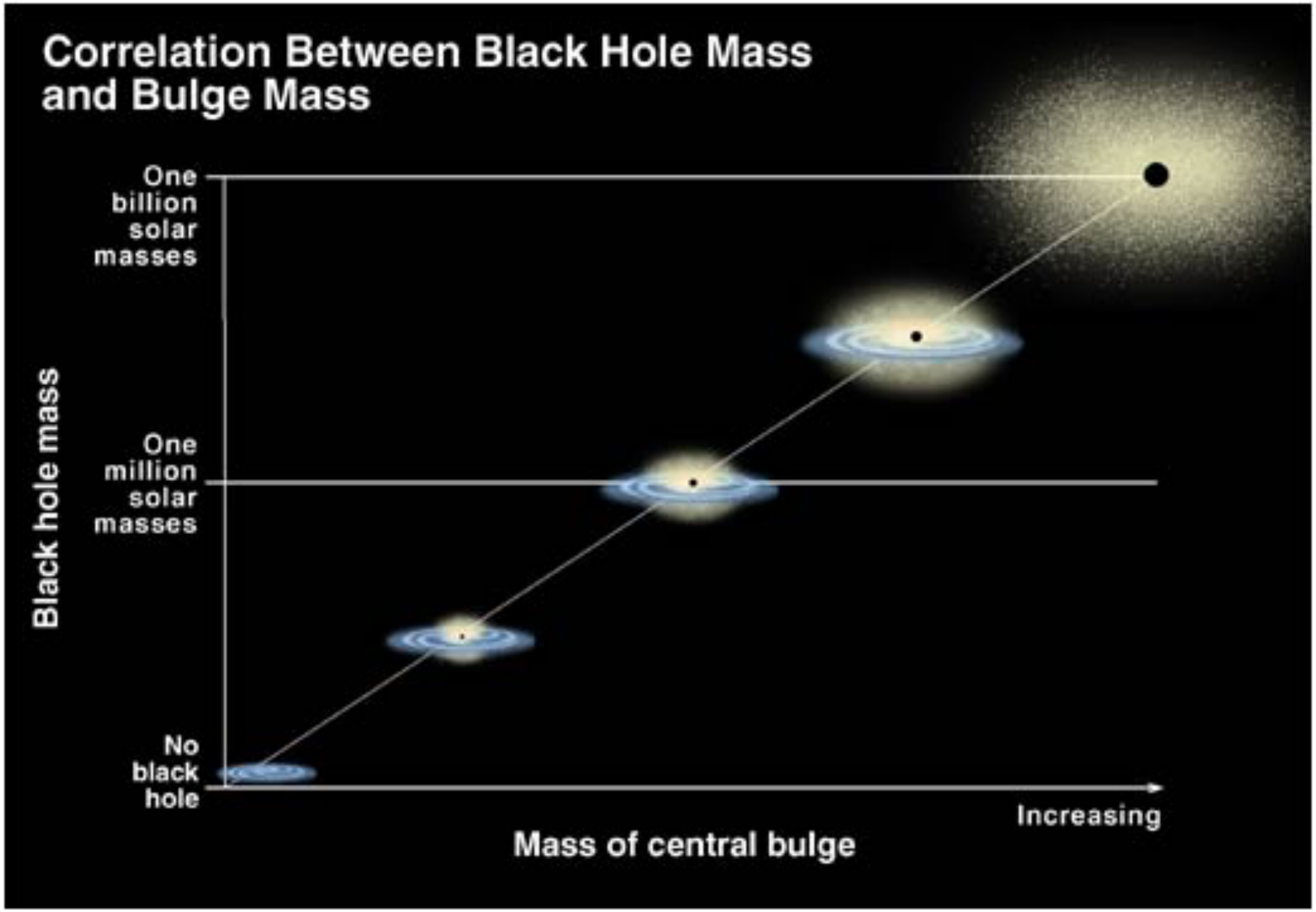

K. Cordes & S. Brown (STScI)

Feedback

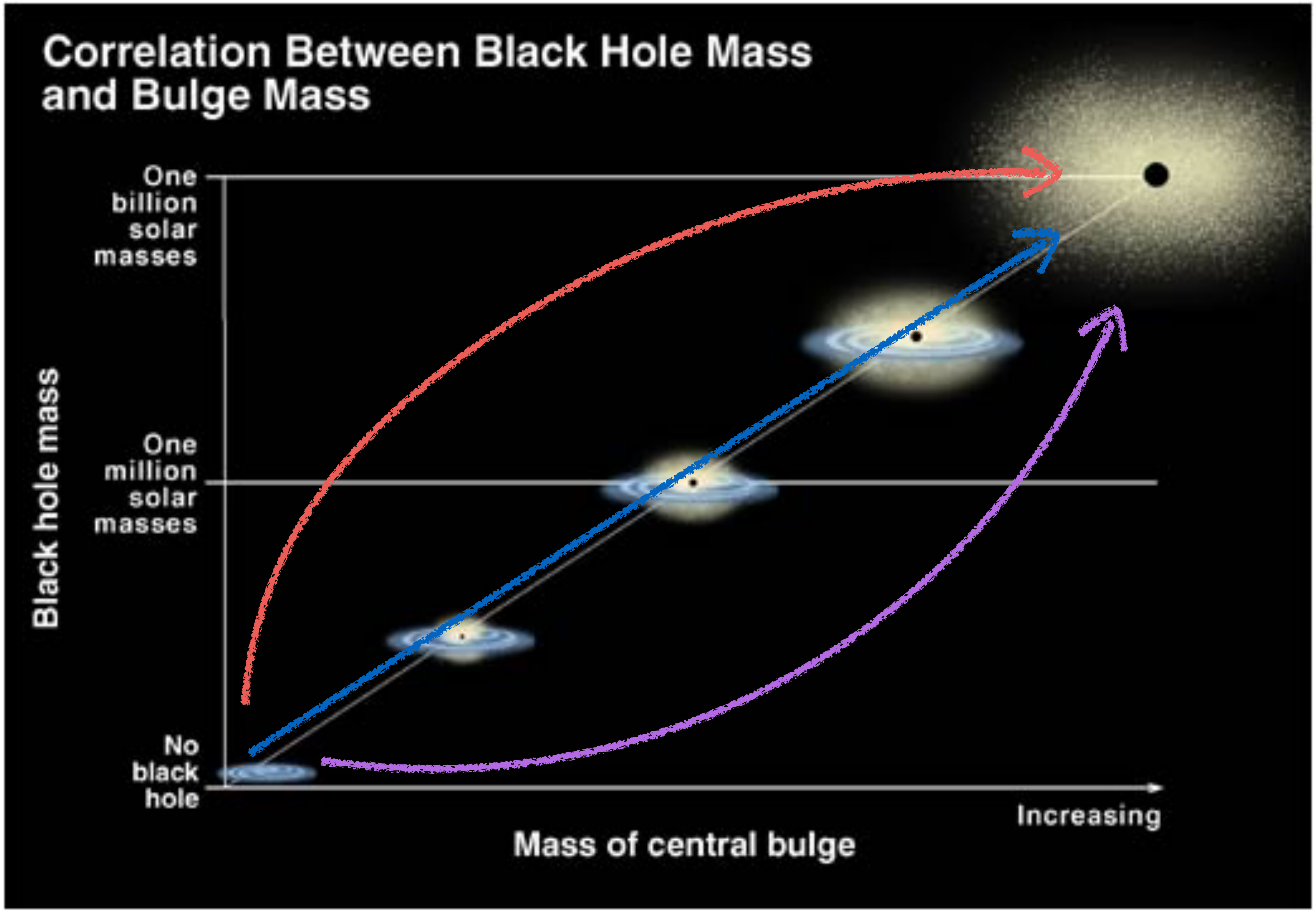

K. Cordes & S. Brown (STScI)

Optical follow-up

Next step: Need spectroscopic confirmation

Spectroscopy:
- Within 2'' of X-ray position find 7753 objects of 11671, 318 have spectra 49/318 have velocities +-5000 kms^{-1}

Imaging:
- Quantify asymmetries and close pairs in spectroscopically confirmed cluster members

Spectroscopy

VIMOS follow-up program:

Expect: 500-700 targets per cluster (~6000 targets)

~860 X-ray AGN

>50 within ~2x r_{500},

(15 so far)

Matched by magnitude and cluster centric distance for V<23

2700 seconds on target

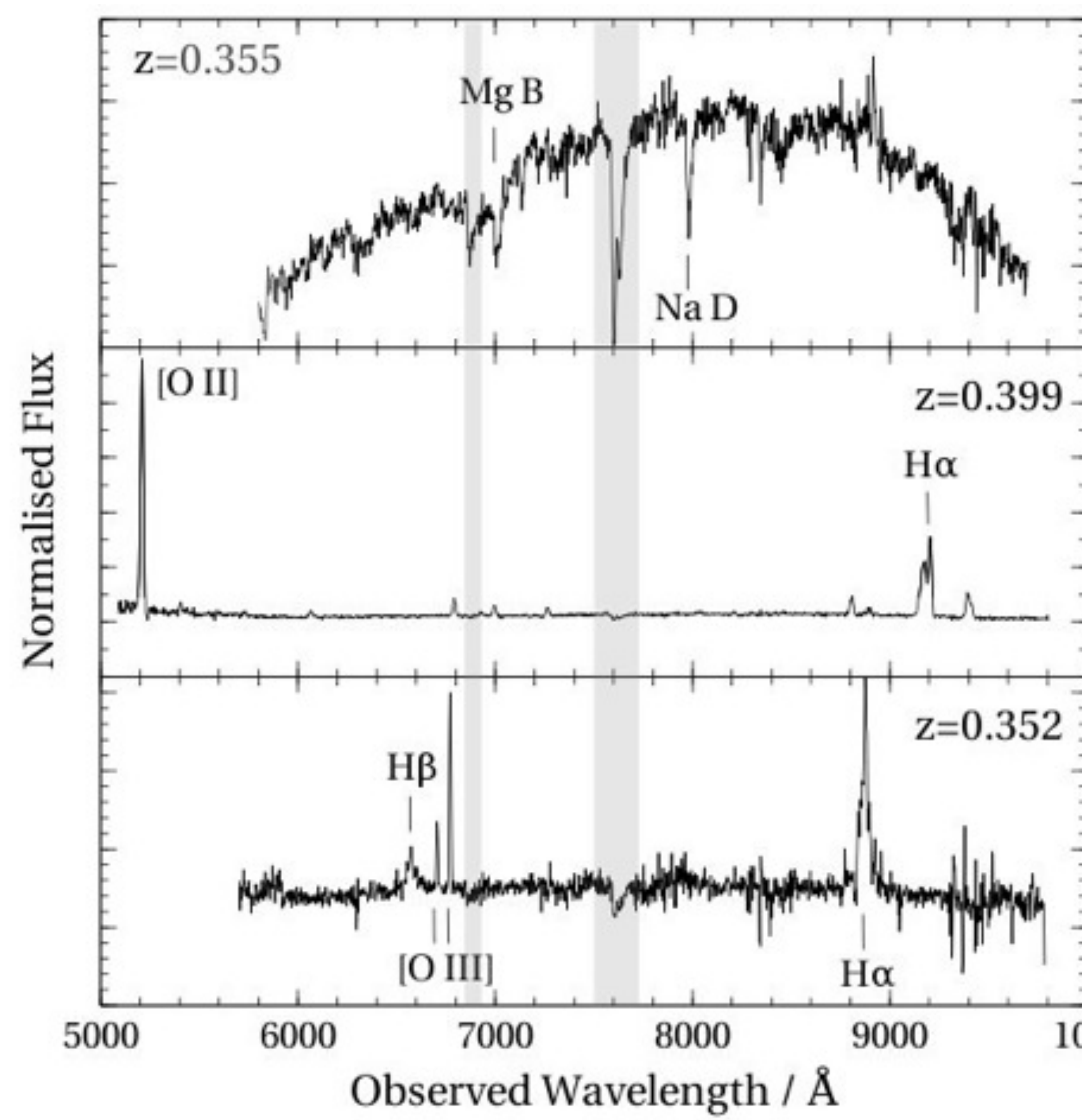

Merger Rates

- Rate of Mergers Scales inversely with the Mass of the most massive Clusters
- $\sigma^3 \propto M^{-1}$
- (e.g., Mamon 1992)
- Though the X-ray AGN are quenched in clusters, the ones that are active are consistent with being triggered by merging of galaxies.

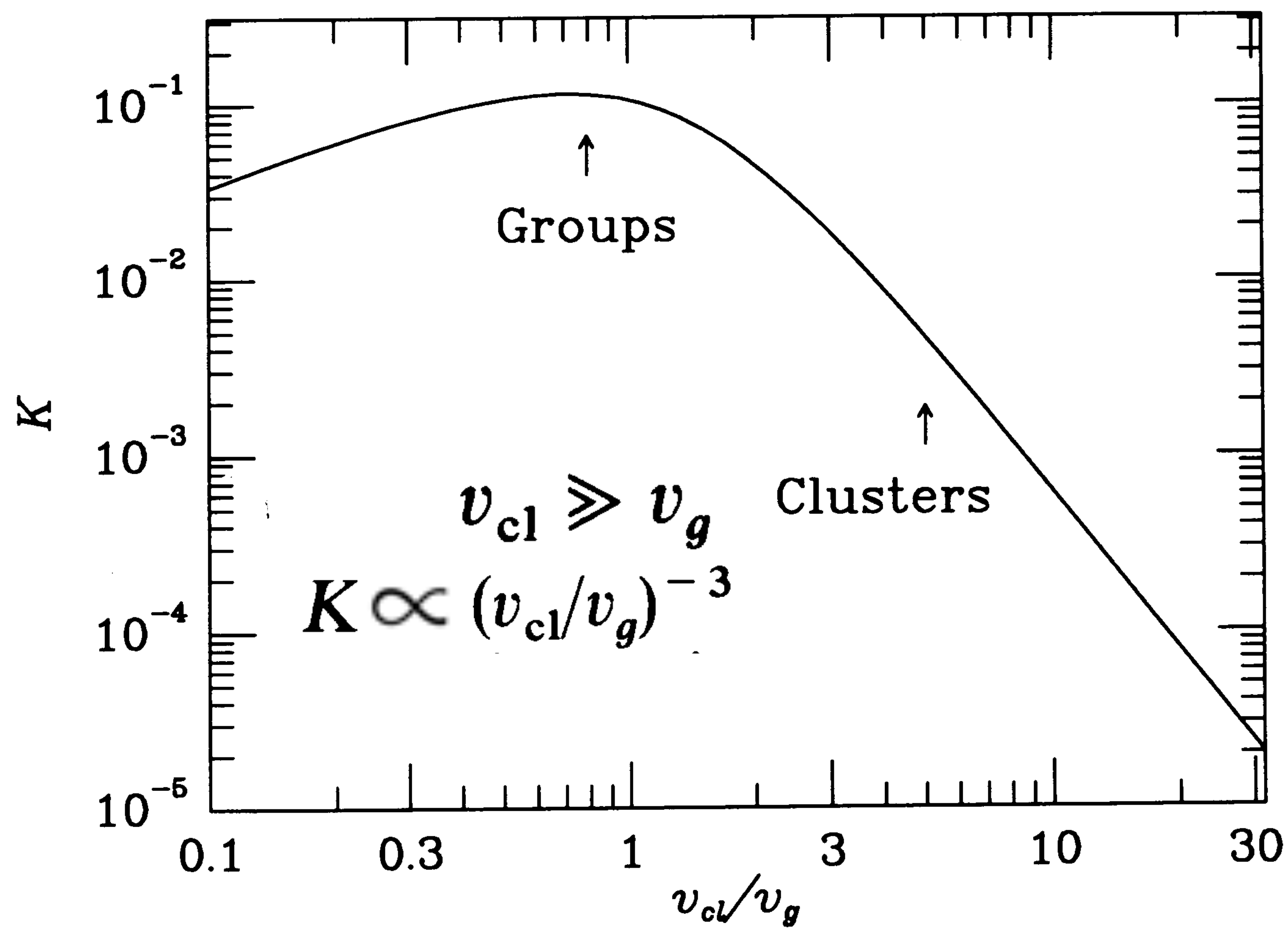

Motivation

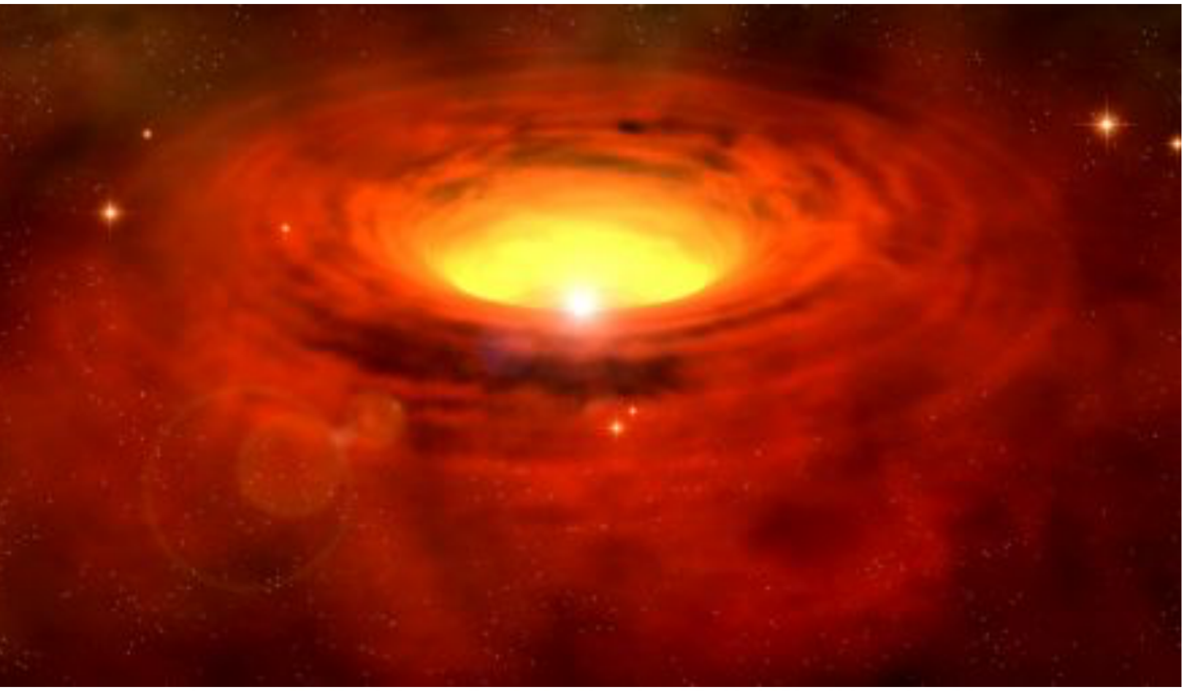

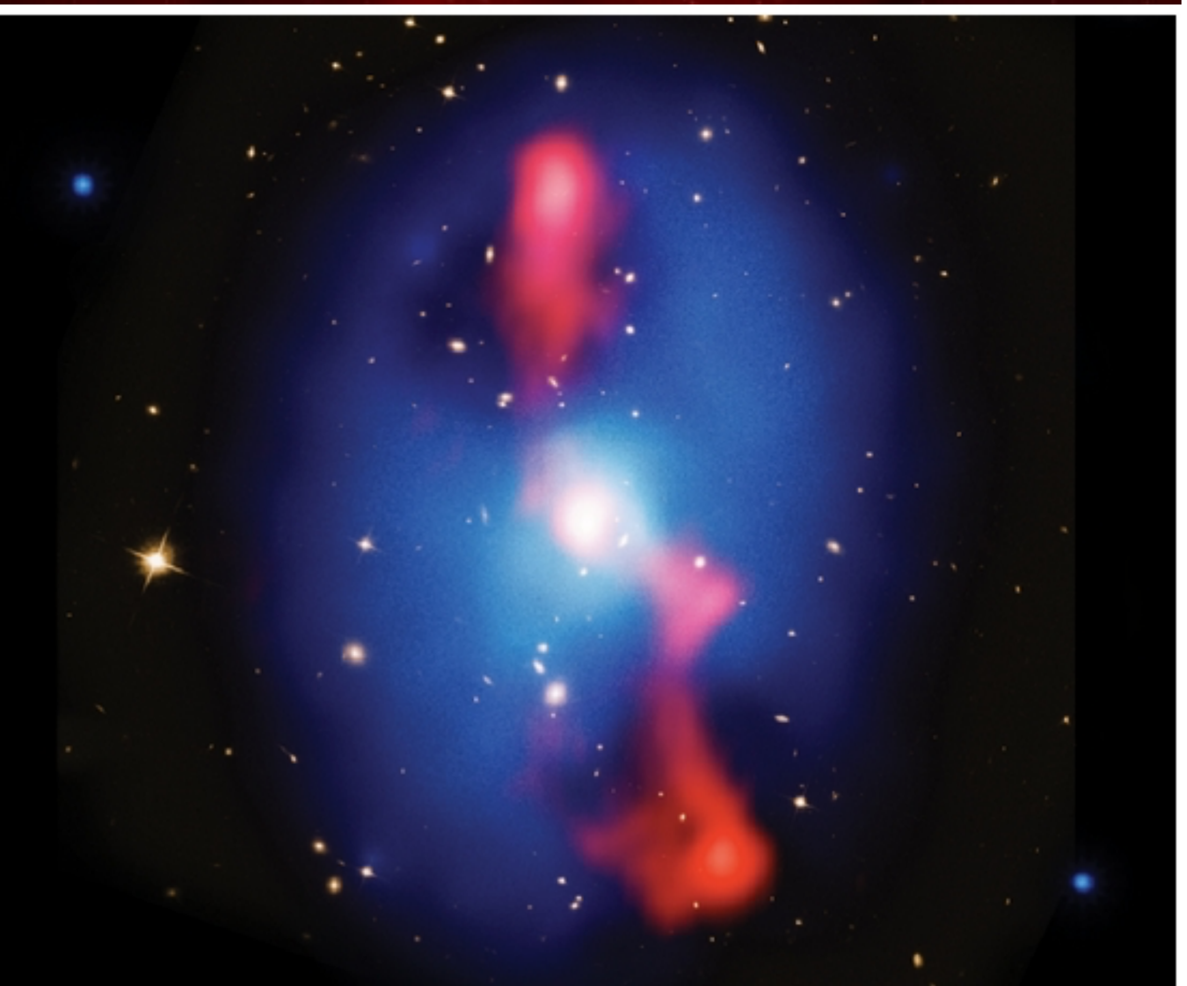

AGN Come in Two Flavors:

- Radiative, Quasar mode, high-Eddington accretion modes (X-ray AGN)
- Kinetic, Jet-mode, low-Eddington accretion modes (Radio AGN)

Feedback

M-sigma Relation

Gultekin et al. 2009

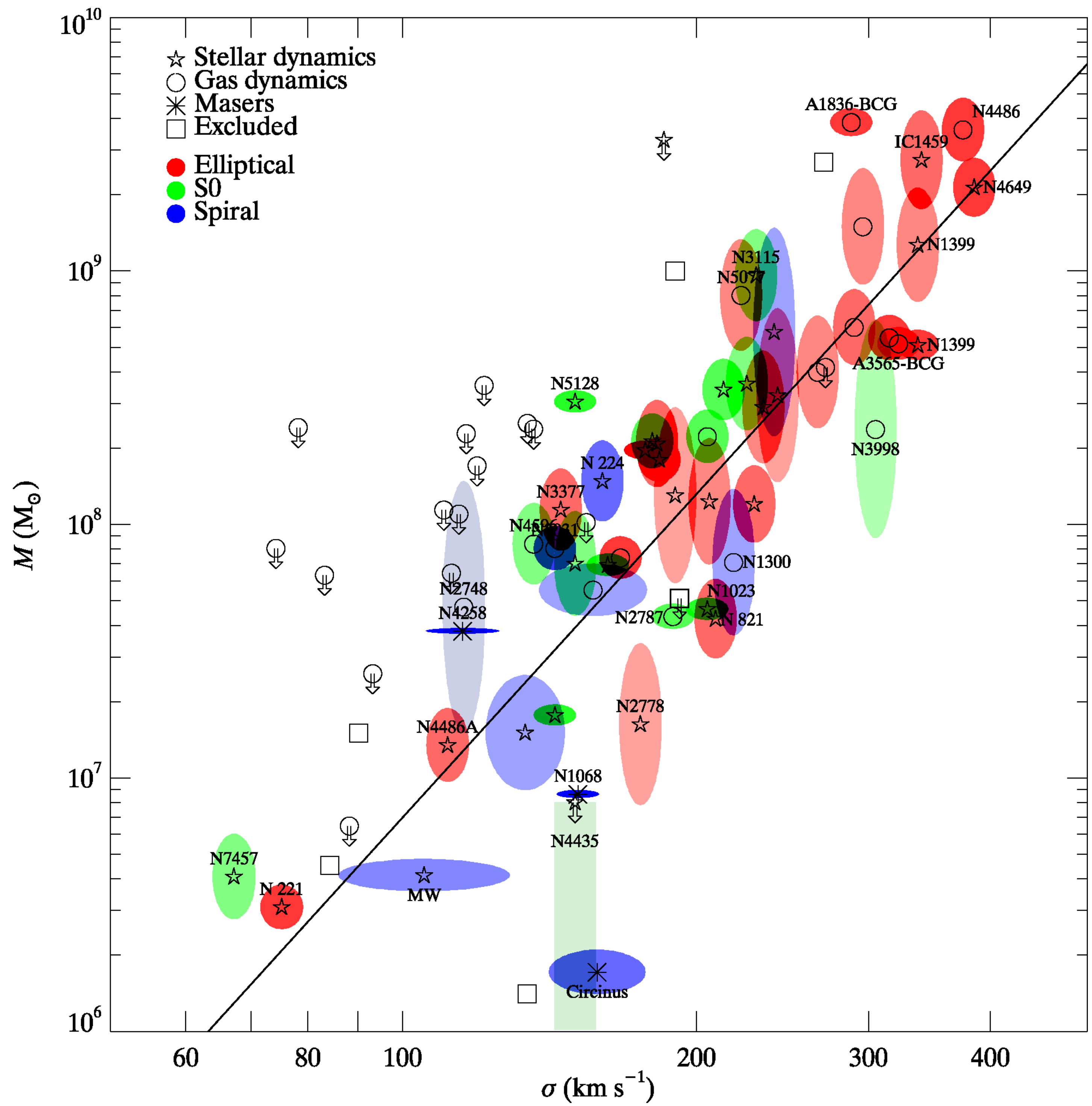

- Sphere of influence
  - 40 pc for 10^9 M_{solar} BH
- The velocity dispersions are measured on kpc scales

Motivation

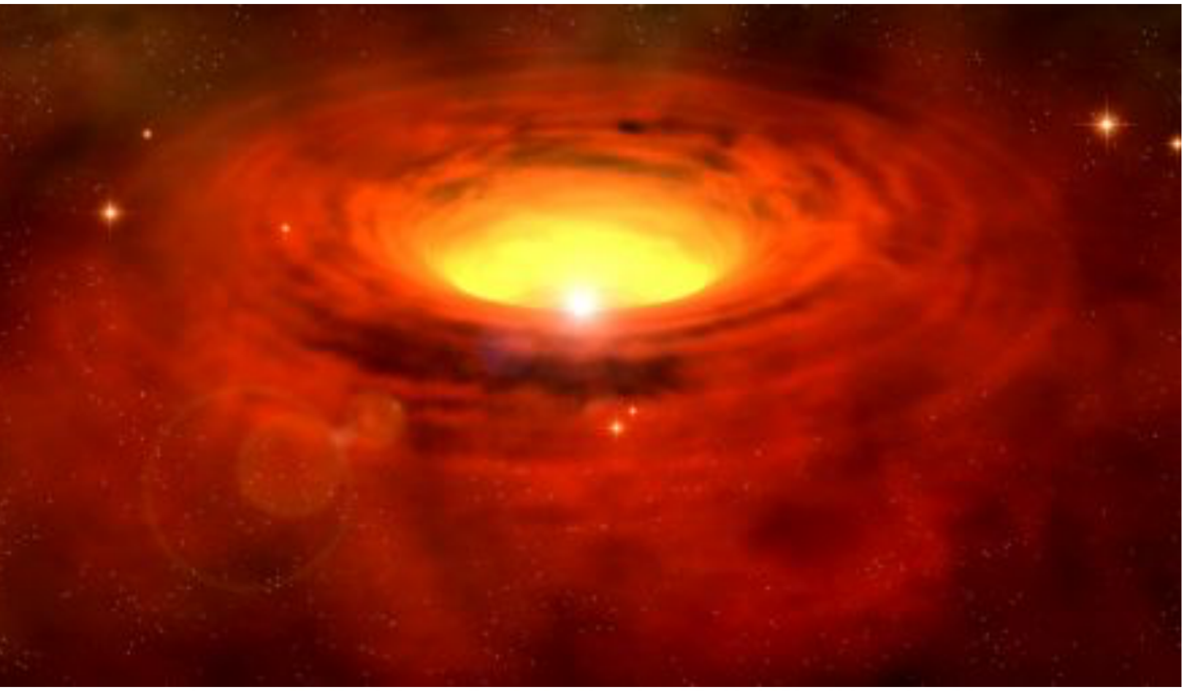

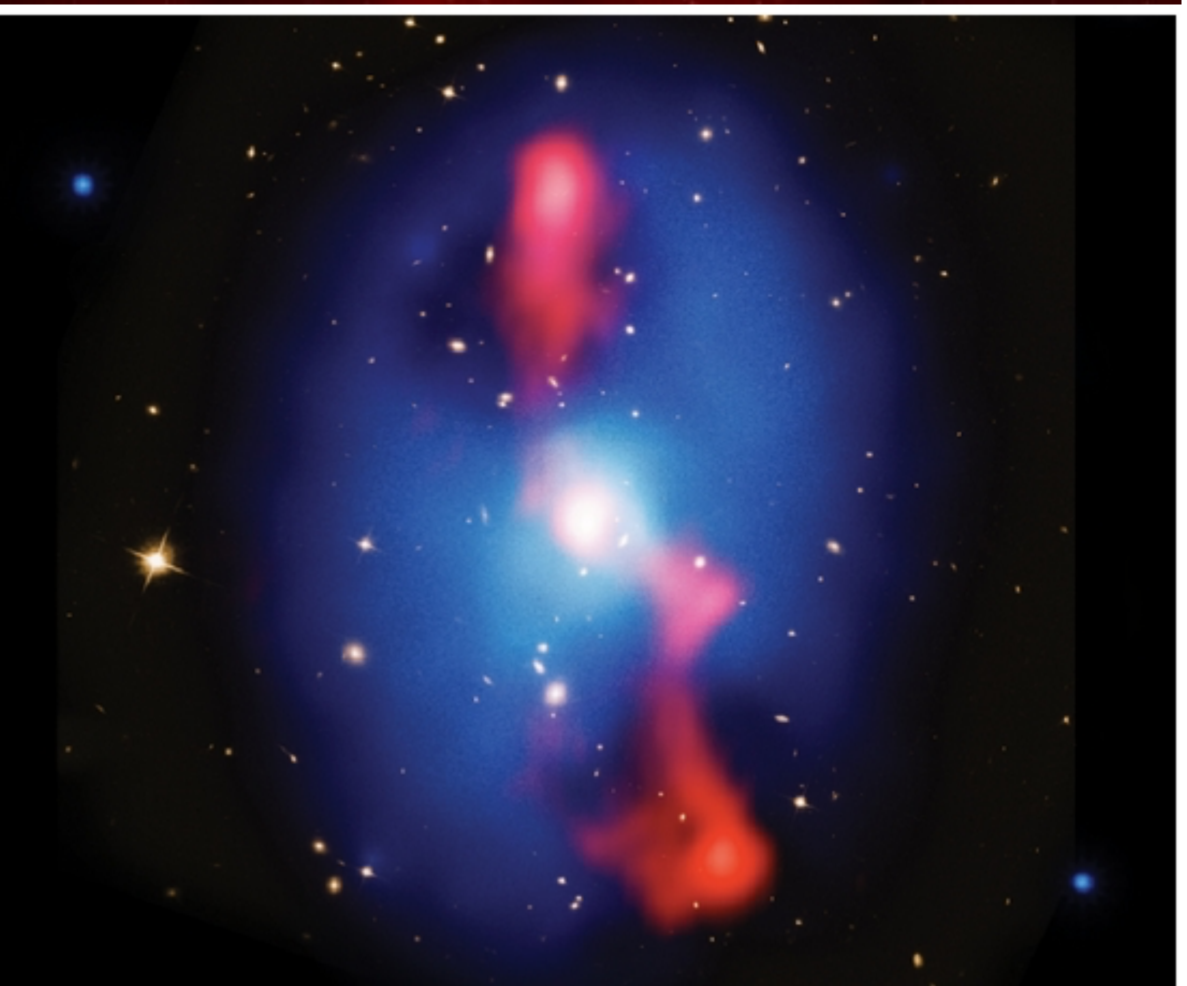

AGN Come in Two Flavors:

- Radiative, Quasar mode, high-Eddington accretion modes (X-ray AGN)
    - measure power:
        - Radiation pressure-luminosity
- Kinetic, Jet-mode, low-Eddington accretion modes (Radio AGN)
    - measure power:
        - Cavities

Motivation

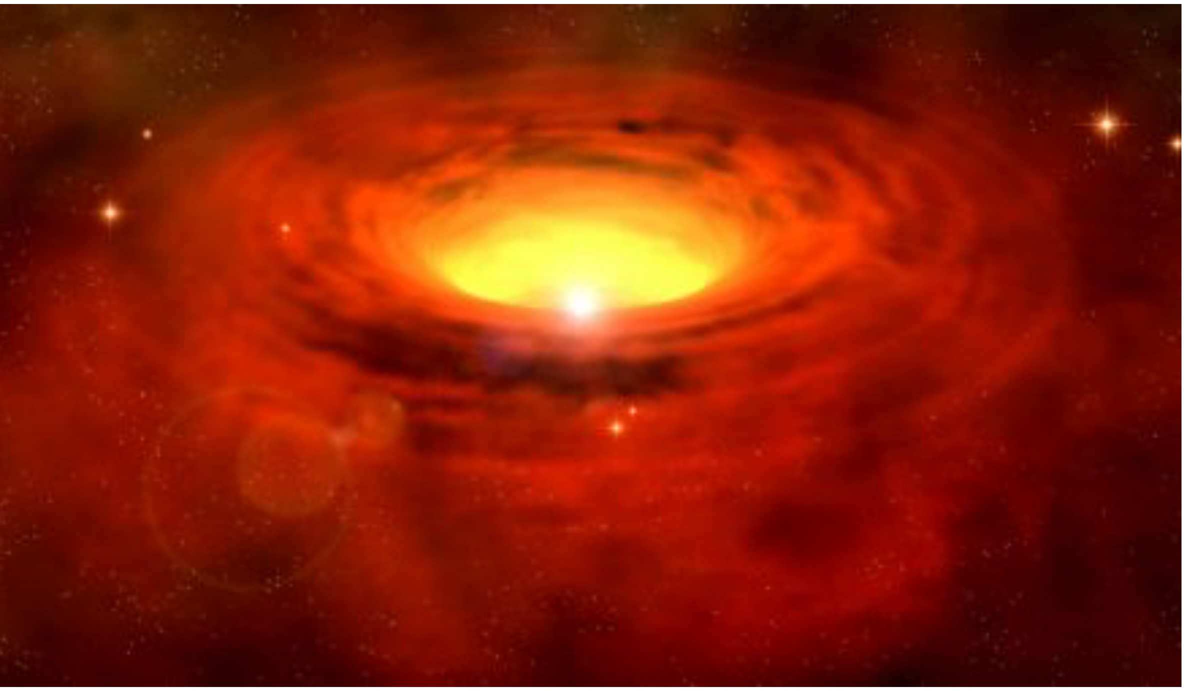

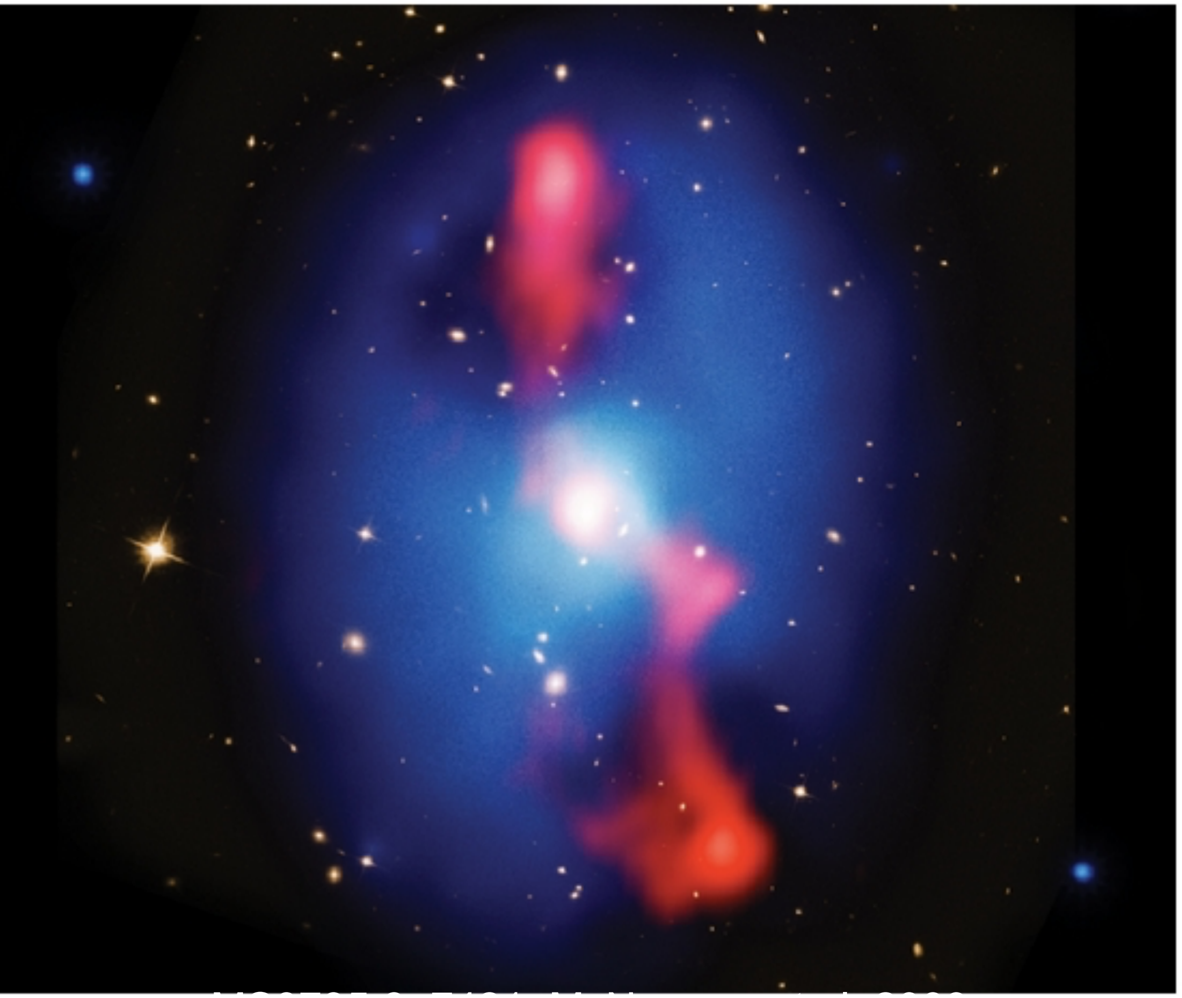

AGN Come in Two Flavors:

- Radiative, Quasar mode, high-Eddington accretion modes (X-ray AGN)
- Kinetic, Jet-mode, low-Eddington accretion modes (Radio AGN)

What are the triggering mechanisms?

X-ray AGN Number Density

- Excess in the center R500 above a luminosity of logL_X=43.5 at the cluster redshift
- The fraction of X-ray AGN compared to galaxies is suppressed as compared to the field
- We find an inverse correlation with Mass, which may suggest triggering of AGN by Mergers